Deltares

Enabling Delta Life

Validation of SWAN wave directions

Deltares

Validation of SWAN wave directions

Joana van Nieuwkoop
Caroline Gautier

1220082-007

Deltares

Title
Validation of SWAN wave directions

Client	Project	Reference	Pages
RWS - WVL	1220082-007	1220082-007-HYE-0003	51

Keywords
SWAN, wave directions, validation, hindcast

Summary
In this report the SWAN performance in complex tidal inlet systems regarding wave directions for storm conditions was studied for SWAN runs in stationary mode. In addition, it was investigated what the SWAN accuracy concerning wave directions implies for the hydraulic loads and the required crest height.

The performance of the SWAN mean wave direction was studied in a statistical error analysis using the results of existing hindcast studies in the Amelander Zeegat, the Eastern Wadden Sea and the Western Scheldt. Close to the coast there are limited directional measurements available. However, the few observations show that SWAN biases of 10 to 20 degrees in the mean wave direction are likely with a standard deviation of circa 5 degrees. In addition, the directional spreading is underestimated with 10 to 20 degrees and the standard deviation is a few degrees. The agreement between the computed and measured mean wave directions is better in cases where wind-sea predominates than in cases where low-frequency wave penetration is measured.

Besides analysing the SWAN performance, it was investigated what the SWAN accuracy concerning wave directions implies for the hydraulic loads and the required crest height. This was done by studying the sensitivity of the results of wave overtopping calculations in Hydra-K to changes for wave direction, using the CR-2011 database. The sensitivity analysis showed that the effect of an error in the wave direction is largest when the angle of wave attack is larger than 75^{o} w.r.t the dike normal. Furthermore, the hydraulic loads seem to be very sensitive to the inclusion of a secondary wave direction in the load function when the angle of wave attack of the primary wave direction relative to the dike normal is larger than circa 60^{o} w.r.t the dike normal.

Furthermore, with the help of an existing study for the Amelander Zeegat it was investigated how sensitive the wave direction near the Frisian coast behind Ameland is to SWAN input and physical settings. In addition a number of extreme storm events from the CR-2011 database (in the order of 1/4000 year return periods) were examined to get an idea which stretches of coast are likely to be attacked by locally generated wind-sea and which by mixed swell and wind-sea conditions. The reason for this is that the sensitivity study for the Amelander Zeegat showed that in areas where wind-sea predominates, the wave direction near the water defences will be mainly sensitive to directional information in the imposed wind fields. However, at locations where the low-frequency wave penetration is relatively high (where tidal inlets are wide and the foreshore is steep) the mean direction will be influenced by other factors as well (e.g. model inputs and other model physics) and errors in the wave direction are likely to be higher. It should be noted that these findings should be handled with care, as all conclusions are solely based on SWAN computations.

Based on the analyses performed in this study, it was concluded that the locations in complex tidal inlet systems where the largest errors in hydraulic loads are expected are the areas where:
- The angle of wave attack w.r.t. the dike normal is large;

Deltares

Title
Validation of SWAN wave directions

Client	Project	Reference	Pages
RWS - WVL	1220082-007	1220082-007-HYE-0003	51

- A high low-frequency wave penetration is expected.

An indicative maximum error in required crest height of plus or minus 35 to 70 centimetres could be expected, in case both aspects occur.

It is recommended to perform more directional measurements near the coast to confirm the results presented in this report. Furthermore, more research is necessary into the effect of bi- or multi modal sea states on the hydraulic loads.

Version	Date	Author	Initials	Review	Initials	Approval	Initials
1	Oct. 2015	Joana van Nieuwkoop Caroline Gautier		André v.d. Westhuysen		Marcel van Gent	
2	Nov. 2015	Joana van Nieuwkoop Caroline Gautier	JvN	Jacco Groeneweg		Marcel van Gent	

State
final

Contents

Samenvatting (summary in Dutch)

In dit rapport is onderzocht hoe goed het golfmodel SWAN, wanneer het model stationair gedraaid wordt, de golfrichtingen voorspelt in complexe getijdebekkens tijdens stormcondities. Daarnaast is bekeken hoe gevoelig de berekeningen van de hydraulische belasting en de benodigde kruinhoogte zijn voor fouten in de golfrichting.

Met een statistische foutenanalyse is gekeken in hoeverre SWAN de gemiddelde golfrichting juist voorspelt. Hierbij is gebruik gemaakt van bestaande hindcast studies in het Amelander Zeegat, de oostelijke Waddenzee en de Westerschelde. Nabij de kust is het aantal richtingsmetingen helaas beperkt. Echter, de validatie met de beschikbare richtingsmetingen nabij de kust toont dat de model bias van de gemiddelde golfrichting in SWAN tussen de 10 en 20 graden ligt met een relatief kleine standaard deviatie van circa 5 graden. De prestaties van SWAN zijn beter wanneer windgolven dominant zijn dan wanneer er ook een significante laag-frequente golfcomponent aanwezig is.

De gevoeligheid van de berekeningen van de benodigde kruinhoogte voor fouten in de golfrichting is onderzocht door de golfrichting te variëren in de golfoverslag berekeningen in Hydra-K, gebruik makend van de CR-2011 database. De gevoeligheidsanalyse toont aan dat het effect van een fout in de golfrichting op de kruinhoogteberekening het grootst is wanneer de hoek van golfaanval groter is dan 75^o ten opzichte van de dijknormaal. Ook is een analyse uit voorgaande rapporten gepresenteerd die toont wat de invloed is op de hydraulische belasting wanneer een deel van de golfenergie uit een andere golfrichting komt dan de primaire golfrichting (zogenaamde bi-modale golven). Uit deze analyse is gebleken dat het effect van bi-modale golven op de hydraulische belasting groot is wanneer de hoek van inval van de primaire component groter is dan 60^o ten opzichte van de dijknormaal, maar klein is bij kleinere hoeken van golfinval.

Tot slot is op basis van een bestaande studie voor het Amelander Zeegat bestudeerd hoe gevoelig de golfrichting nabij de Friese kust achter het Amelander is voor SWAN invoer en fysische instellingen. Ook zijn de SWAN resultaten voor een aantal extreme stormen (orde 1/4000 jaar terugkeertijd) uit de CR-2011 database bestudeerd om een idee te krijgen in welke delen in de Waddenzee en Westerschelde significante laag-frequente golfdoordringing plaatsvindt. De gevoeligheidsanalyse voor het Amelander Zeegat heeft namelijk laten zien dat wanneer windgolven dominant zijn, de golfrichting nabij de waterkeringen voornamelijk gevoelig is voor de windrichting. Echter, wanneer er significante laag-frequente golfdoordringing optreedt (bijv. bij wijde getijdebekkens) zal de gemiddelde golfrichting ook beïnvloedt worden door andere factoren (bijv. de golfrandvoorwaarden en verschillende model fysica). Daardoor is het waarschijnlijker dat de fouten in de golfrichting groter zijn wanneer significante laag-frequente golfdoordringing tot de dijk optreedt dan wanneer lokaal opgewekte windgolven domineren.

Wanneer de resultaten van de verschillende analyses uit deze studie worden gecombineerd kan worden geconcludeerd dat de grootste fouten in de hydraulische belasting/benodigde kruinhoogte kunnen worden verwacht in gebieden in het getijdebekken waar:

- De hoek van golfinval schuin is (groter dan 75^o ten opzichte van de dijknormaal);
- Een grote hoeveelheid laag-frequente energie wordt verwacht.

Een indicatie voor de maximale fout in de benodigde kruinhoogte is plus of min 35 – 70 centimeter indien beide bovengenoemde aspecten op de locatie voorkomen.

Het verdient de aanbeveling om meer golfrichtingsmetingen nabij de kust uit te voeren om de resultaten uit deze studie te bevestigen. Daarnaast is het noodzakelijk om meer inzicht te krijgen in de invloed van bi-modale golven op de hydraulische belastingen.

List of Tables

List of Figures

1 Introduction

1.1 Framework

In compliance with the Dutch Water Act ("Waterwet, 2009") the strength of the Dutch primary water defences must be assessed periodically for the required level of protection, which, depending on the area, varies from 300 to 100,000 year loads in the assessment round of 2017. These loads are determined on the basis of Hydraulic Boundary Conditions (HBC). The HBC and the Safety Assessment Regulation ("Voorschrift op Toetsen op Veiligheid", VTV), play a crucial role in the assessment of the primary water defences.

With the aim of delivering legal assessment instruments to be used in the fourth assessment period, starting in 2017, DGRW is funding the long-term project WTI 2017, with Rijkswaterstaat – WVL as executive client for Deltares. One of the objectives of WTI 2017, besides delivering HBC, is to fill in the most important knowledge gaps concerning Hydraulic Loads, in such a way that from 2017 onwards more reliable HBC for the Dutch primary sea and flood defences can be determined. The study reported here, whose motivation is given in the next section, focuses on the knowledge gap regarding the wave model SWAN.

1.2 Motivation

For the WTI calculations of the Hydraulic Boundary Conditions, wave statistics obtained at deeper water buoys need to be transformed to the toe of the dike using the SWAN wave action model (Booij et al., 1999). This is currently done by running SWAN in stationary mode. This transformation is challenging in complex tidal inlet systems such as the Wadden Sea and the Western Scheldt in the Netherlands.

The model performance of SWAN in these areas has often been assessed in hindcast studies, comparing model results with observations. In these hindcast studies usually a lot of attention has been given to the one-dimensional energy density spectrum and the integral wave parameters: significant wave height and mean period. However, the wave directions have been less well validated. Also, directional wave measurements are scarce in many study areas and especially close to the water defences, which makes it hard to validate the wave directions.

Nonetheless, the wave direction and especially the directional distribution are very important for wave modelling. The directional distribution of low-frequency waves (<0.1 Hz) determines how far and wide the waves will disperse. Moreover, as has been shown in Deltares (2014a), the prediction of low-frequency energy wave penetration is influenced by non-linear interactions and refraction. For these processes the wave direction plays an important role. Therefore, comparing the modelled and observed directional distributions and modelled and observed (radar) spatial distributions in Deltares (2014a) has proven to be valuable in identifying discrepancies between SWAN and the measurements.

The wave direction is an important aspect in the wave propagation and hence for the amount of wave energy that reaches the coast. The ebb-tidal delta and channels can have a large influence on the wave direction and thus on the propagation. A local error in modelled wave direction could therefore result in an under- or overestimation of the amount of wave energy near the coast, possibly leading to less reliable hydraulic boundary conditions.

Finally, the quality of the computed wave directions in front of the primary water defences is important as the wave angle with respect to the dike orientation is taken into account in the assessment of run-up, overtopping and the revetment characteristics. Errors in the computed wave direction could influence these calculations. Furthermore, the wave direction is one of the three parameters that can influence the load function of the probabilistic calculation for some failure mechanisms, which has an effect on the representative load that is used for the assessment.

1.3 Objectives

The aim is to assess the SWAN performance, when run in stationary mode, in complex tidal inlet systems regarding wave directions for storm conditions. Furthermore, it is aimed to assess what the SWAN accuracy concerning wave directions could imply for the hydraulic loads and the required crest height.

With these objectives, an indication is given for the error that is made in the required crest height due to possible errors in wave direction and in which areas large errors in required crest height are likely to occur. This study can be seen as a first step in defining the uncertainty of the SWAN wave direction in the hydraulic boundary conditions. The study area is limited to areas where directional wave observations are available, being the Wadden Sea and the Western Scheldt.

1.4 Approach

The following steps will be taken to study the SWAN performance regarding the wave direction for storm conditions:

1 Literature study existing hindcasts
An overview will be made of the conclusions of existing studies in the Amelander Zeegat, the Eastern Wadden Sea and the Western Scheldt regarding the wave direction. The focus for this analysis will be on the statistical agreement between the computed and observed directional parameters (mean wave direction and directional spreading). With this step an idea of the SWAN performance regarding wave direction is gained for different study areas, locations and storms.

All the hindcast runs that are used were run in stationary mode and the hindcast time instances were carefully selected for stationary conditions. As the HBC of WTI2017 are determined for instances rather than time evolving storms, the directional performance of the stationary runs presents a good measure of the performance of the HBC runs.

2 Sensitivity of hydraulic loads/ required crest height to wave direction
Additionally, the question is addressed how sensitive the hydraulic loads are to the wave direction. This will be done by studying the sensitivity of the wave run-up and overtopping formula for wave direction and in addition the load function.

3 Sensitivity of the wave direction to the wave conditions, model inputs and physics
Based on literature, it is investigated to what extend variations in wave direction in the ebb-tidal delta influence the mean wave direction along the dikes. This is done by looking at the sensitivity of the results near the coast to different SWAN inputs and physical settings. Furthermore, the wave conditions near the dikes are studied during extreme storms (order 1/4000 year return period).

1.5 Outline of the report

The outline of the report is as follows: in chapter 2 existing hindcasts are analysed. Subsequently in chapter 3 the sensitivity of the hydraulic loads/required crest height to wave direction is analysed and in chapter 4 the sensitivity of the wave direction to different model inputs and physics is examined. Subsequently in chapter 5 it is attempted to give an indication of the error in required crest height with the analyses of chapters 2, 3 and 4. Finally in chapter 6 conclusions and recommendations are given.

2 Quality of SWAN wave directions based on existing studies

2.1 Introduction

In this chapter, the SWAN performance regarding wave direction is assessed, making use of existing hindcast studies. The following hindcasts are available from studies performed over the last decade: 26 cases for the Amelander Zeegat (Section 2.2), 11 cases in the Eastern Wadden Sea (Section 2.3) and 30 cases in the Western Scheldt (Section 2.4). Hydrodynamic models (Delft3D or WAQUA) were used to predict the water levels and currents for the hindcasts. The model resolution of the different hindcast studies was based on the variation in bathymetry and resulting variation in wave height. All hindcasts considered for the statistical comparison used WTI settings and SWAN model version 40.72ABCDE, to be able to make a fair comparison. These settings were also used for the WTI 2011 production runs. The WTI settings are:

- Quadruplet interactions using the DIA formulation by Hasselmann et al. (1985).
- JONSWAP formulation for bottom friction with a coefficient set to 0.038 m^2s^{-3} for fully developed wind-sea conditions in shallow water, as found by Bouws and Komen (1983).
- Depth-induced breaking under finite-depth wave growth conditions (Van der Westhuysen, 2009, 2010), model parameter settings: B = 0.96, β_{ref} = -1.3963, v = 500.
- Triad interactions using the LTA formulations by Eldeberky (1996): trfac=0.1
- Wind generation and whitecapping based on Van der Westhuysen et al. (2007), but corrected for an underprediction of swell (Van der Westhuysen, 2007).
- Enhanced whitecapping dissipation on negative current gradients according to Van der Westhuysen (2011), model parameter setting C_{ds}''= 0.8.
- 80 iterations for complete convergence.
- The quadruplets are de-activated for Ursell numbers larger than 10 (Ursell limiter). The threshold for fraction of breaking waves is set to 1.

In this reanalysis the focus is on the statistical comparison of the computed and observed parameters for mean wave direction and directional spreading. For every area the directional statistics have been calculated for all hindcast time instances and locations together and for every storm/location separately. The statistical parameters used in this analysis have been explained in Appendix A. Additionally, any remarks or further analyses on the wave direction in previous studies have been briefly summarized in the following sections. Finally, in Section 2.5 the main conclusions from the analysis in this chapter have been presented.

2.2 Amelander Zeegat

2.2.1 Hindcasts

The Amelander Zeegat has been extensively studied in several wave hindcast studies in the period 2004 – 2013 (see WL & Alkyon 2007a, Alkyon 2007a,b, Royal Haskoning 2008, Witteveen+Bos 2008 and Deltares 2014a,b), making use of recent measurement campaigns. Figure 2.1 shows the wave measurement locations that were present in the year 2013. Wave directions are measured at AZB11, AZB12, AZB21 (no data at 5/6 Dec 2013), AZB31, AZB32, AZB41, AZB42, AZB52 (shown with the magenta dots). In the period 2004 to 2013 the locations of some of the buoys have changed considerably. Buoy AZB21 moved further northwards; to make sure it was still located in the channel. In the period 2004-2005 AZB31 was located on the eastside of the channel, being placed there for redundancy. Therefore the buoy information over this period is not taken into account in the statistical analysis. Buoy

AZB31 was moved to the tidal flats on the west side of the channel in 2007 and eventually in 2013 the buoy was located inside the main channel, as has been shown in Figure 2.1. In 2004 AZB41 and AZB51 were located at the location of the 2007-2013 AZB42 respectively AZB52 location. The results for 2004 at these locations have been added to the 2007-2013 AZB42 respectively AZB52 results.

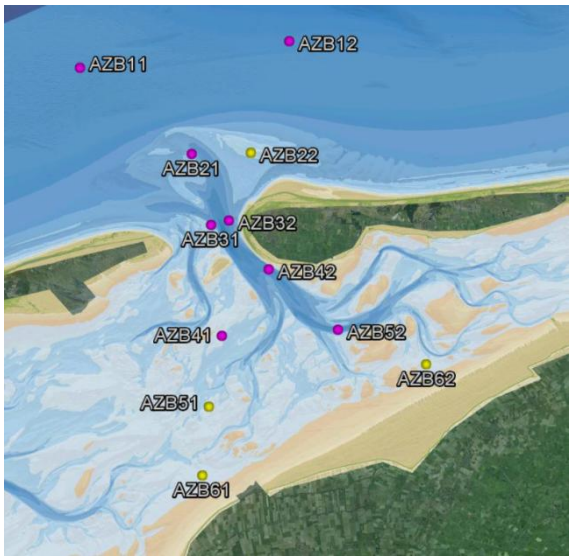

Figure 2.1 2013 wave measurement locations in the Amelander Zeegat. Directional wave information is available at the magenta locations.

Table 2.1 gives an overview of the different hindcast time instances that have been used in the statistical analysis of the wave directions. The hindcast time instances from 2004 to 2007 have been reported in Deltares (2011). It should be noted that the wave hindcast of December 2005 was omitted from this table, as the measured wave directions showed unrealistic values. The results of the hindcasts were taken from the SWIVT database (SWAN Instrument for Validation and Testing, Wenneker et al. 2009) which contains not only the observations but also the results from the SWAN runs with WTI settings as required for the present study. These settings have also been applied in the December 2013 hindcast (not yet available in SWIVT), but without the Ursell limiter.

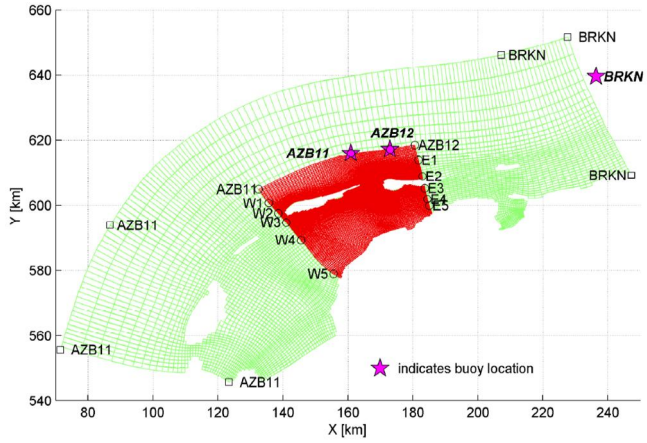

Figure 2.2 An example of the grids used in the December 2013 hindcast. Grids G1 (green and G2 (red) (every 3rd grid line) and locations for wave boundary conditions. As presented in Deltares (2014b)

In all cases a large grid, covering part of the Wadden Sea, is used to translate offshore waves to the boundary of a smaller Amelander Zeegat grid, see for example the grids that were used in Deltares (2014b) in Figure 2.2. At the Amelander Zeegat grid the measured spectra of AZB11 and AZB12 are applied as boundary condition. Therefore, in the statistical analysis in the next section the SWAN results of the large grid are used to compare the measurements at AZB11 and AZB12 to the SWAN results. For the other locations, only the results at the Amelander Zeegat grid are considered.

	Hindcast time instance	U_{10} (m/s) mean over domain	Udir (°N) mean over domain	Wl (m + NAP) at station Nes	umax (m/s) in the inlet main channel	Tidal phase
1	08/02/2004, 20:00	13.5	314	1.0	2.3	flood
2	08/02/2004, 22:30	16.6	325	2.6	0.9	high w
3	09/02/2004, 01:30	16.3	328	1.8	1.7	ebb
4	11/01/2007, 13:00	19.5	228	1.0	0.7	high w
5	11/01/2007, 22:00	17.9	275	0.9	0.6	flood
6	11/01/2007, 22:40	18.8	279	1.3	0.7	flood
7	18/01/2007, 12:20	21.1	233	0.8	1.3	ebb
8	18/01/2007, 14:00	20.2	263	0.6	1.0	low w
9	18/01/2007, 17:20	20.3	267	1.4	1.1	flood
10	18/01/2007, 20:40	18.9	274	2.8	1.1	high w
11	18/03/2007, 10:00	13.8	279	1.7	0.4	high w
12	18/03/2007, 14:40	18.1	266	0.7	1.2	low w
13	18/03/2007, 15:40	17.9	271	0.6	0.8	low w
14	18/03/2007, 17:00	17.1	268	1.2	1.1	flood
15	18/03/2007, 19:20	16.3	268	3.0	1.3	flood
16	09/11/2007, 04:50	17.3	322	1.2	1.3	flood
17	09/11/2007, 09:20	18.4	326	2.7	0.7	high w
18	09/11/2007, 11:00	18.5	328	1.7	1.3	ebb
19	05/12/2013, 22:00	22.9	322	3.20	0.5	HW slack
20	06/12/2013, 00:00	24.6	303	3.26	1.1	HW ebb
21	06/12/2013, 06:00	21.5	306	1.68	0.3	LW flood
22	06/12/2013, 08:00	20.7	299	2.64	0.7	Flood
23	06/12/2013, 10:00	21.3	310	3.20	0.3	HW slack
24	06/12/2013, 13:00	18.6	296	2.21	1.5	ebb
25	06/12/2013, 15:00	18.1	310	1.30	1.7	ebb
26	06/12/2013, 18:00	15.0	305	0.26	0.7	LW ebb

Table 2.1 Wind speed, wind direction, water level and maximum current speed at 26 time instances for which a hindcast has been performed for the Amelander Zeegat in previous studies.

2.2.2 Statistical analysis wave direction

For all wave hindcast time instances presented in Table 2.1, statistics of the wave directions compared to the wave measurements have been calculated, see Table 2.2.

With less than 10 degrees bias and standard deviation for the wave direction and the directional spreading, the overall agreement between the directional parameters of SWAN and the measured directional parameters can be considered good. In most cases the wave direction in SWAN is more northerly than observed. In addition, the directional spreading in SWAN is smaller than observed.

As noted by Kuik et al. (1988), the determination of the directional spreading from buoy measurements is very sensitive to noise causing an increase in the amount of directional spreading. In addition, Krogstad (2001) notes that the directional properties of buoy measurements often show erroneous behaviour below the peak frequency. However, the mismatch can also be an indication that in reality the wave field is more directionally spread due to refraction effects than simulated wave fields.

Of the three storms that were hindcasted, the directional parameters of the westerly November 2007 storm are best predicted by SWAN (though it must be said that for this storm the number of data is the highest). For the February 2004 and December 2013 a larger bias and standard deviation in the wave direction is seen. The bias of the February 2004 is larger because location AZB11 and AZB12 were not included. For all three storms the directional spreading is underestimated by SWAN.

When studying the directional statistics for each location, it can be seen that the wave directions and directional spreading are best predicted by SWAN at the outer (offshore) locations AZB11 and AZB12. In the main channel (AZB21, AZB31 2013 location, AZB32 and AZB42) the computed wave direction is often 10-20 degrees more northerly than observed. In addition, the computed directional spreading at these locations is on average 10 degrees lower than observed. Finally, the estimation by SWAN of directional parameters at the locations located on the tidal flats (AZB31 locations 2007, AZB41, AZB52) is less biased than in the tidal channels. This is as expected since the waves are mainly wind driven here. The measured low-frequency energy penetration on the tidal flats is low. This means that - compared to the waves in the tidal channel - the waves are shorter (frequencies usually higher than 0.35 Hz) and thus less influenced by processes that could influence the wave direction, like nonlinear interactions, wave-current interaction and refraction, see also WL&Alkyon (2007b). Location AZB52 is the location closest to the Frisian dikes, but still some 8 km off.

	Wave direction					Directional spreading					
	Bias [°]	stdev [°]	Rmse [°]	X_{mean} [°]	Y_{mean} [°]	Bias [°]	stdev [°]	Rmse [°]	X_{mean} [°]	Y_{mean} [°]	N
All	6.53	5.99	12.35	295	302	-5.35	5.11	8.27	32	27	171
Feb 2004	15.24	6.34	16.55	291	307	-15.2	5.03	15.94	40	25	5
Nov 2007	5.37	5.14	9.54	286	291	-5.83	4.93	8.24	32	27	110
Dec 2013	7.62	7.33	16.2	313	320	-3.55	5.22	7.25	31	28	56
AZB11	0.18	3.57	3.73	307	308	1.08	2.77	3	24	25	23
AZB12	2.71	3.35	4.36	306	308	-0.64	1.5	1.65	24	23	23
AZB21	9.07	5.45	11.83	285	294	-10.6	3.65	11.96	39	28	17
AZB31*)	0.89	5.49	5.99	310	311	-10.7	3.83	11.73	39	29	14
AZB31 **)	17.4	7.6	20.4	318	336	-12.6	4.02	13.2	42	30	8
AZB32	7.41	4.4	12.07	309	317	-2.79	3.12	4.19	34	31	16
AZB41	4.82	4.97	19.3	283	288	-5.79	5.06	8.85	39	33	23
AZB42	12.6	5.6	15.5	279	291	-7.38	5.01	9.94	32	24	26
AZB52	**8.36**	**5.9**	**10.9**	**281**	**289**	**-5.45**	**3.47**	**6.49**	**28**	**23**	**21**

Table 2.2 Statistics for wave direction and directional spreading for the Amelander Zeegat. The locations closest to the coast are made bold.
**) 2007 **) 2013*

2.2.3 Findings with respect to SWAN wave directions at the Amelander Zeegat

In this section, findings from existing studies with respect to SWAN wave directions are summarized. Four topics are considered; radar observations, low-frequency wave penetration, the effect of currents on wave direction and the convergence of wave direction. In this section the focus is on the areas where problems with the prediction of the wave direction were identified. Here these problems are briefly summarized with some examples from the hindcast studies. In the existing hindcast studies these problems have been illustrated in more detail/ with more examples.

Radar

On the half circle covering the area between Ameland and Terschelling radar observations are available with a spatial resolution of circa 300 m x 300 m of current speeds and direction, depth, wave angle and wave length. The radar is especially valuable to study the wave directions in the inlet of Ameland, as has been done in Deltares (2010). The data contains valuable information, but should be used with care. Especially in areas with large bottom gradients the results are less reliable due to spatial averaging on the relatively large grid cells. Also, if the wave heights are small (a few decimetres), the radar gives unreliable values.

In Deltares (2010) the differences between the radar and SWAN directions have been studied for the 28 January 2010 storm, see Figure 2.3. In the left-hand panels, the background colours indicate the total water depth of the SWAN simulations, the black vectors the dominant wave direction[1] by the radar and the red vectors the dominant wave direction by SWAN. The white vectors are the peak wave directions by SWAN which are often similar to SWAN's dominant direction. Also, the buoys and the peak direction of the buoys are given. The contours (both in left-hand and right-hand panels) present the position of the seabed, they are equal for all time instances considered. In the right-hand panels, the dominant

[1] *The dominant wave direction is the direction of the energy bin with maximum energy as function of direction and frequency.*

direction from SWAN is subtracted from the radar wave direction, after both were interpolated onto the same grid.

It is seen that the majority of the area, especially outside of the inlet, shows merely small differences within 10 degrees. However, moving into the inlet some large differences of more than 50 degrees in wave direction are found. At X=171 km, Y=609.5 km (see the upper circle), during flood (t1, upper panel) the radar vectors point to the south, whereas the SWAN vectors have an easterly direction. During ebb (t6, lower panels) the differences are limited in this area. The differences in the channel at X=169 km, Y=608-609 km occur predominantly during flood (t1, upper panel). Here the radar indicates that the dominant waves propagate from west-northwest to east-southeast whereas SWAN computes that the waves travel to the east/east-northeast. Further south (X=169 km Y=ca. 607.5, see the lower circle), there is a region of agreement during flood (t1, upper panel) where both SWAN and the radar indicate that the waves to propagate to the east, crossing the channel. During ebb however (t6, lower panel), the SWAN wave direction in the lower circle is more to the south, whilst according to the radar the waves cross the channel here during ebb as well.

In Deltares (2014a) the radar data of the December 2013 storm were compared to the SWAN results, see e.g. Figure 2.4 for hindcast moment 5-12-2013 22:00 (HW). It is seen that during high water the computed waves follow a south easterly direction, whereas the radar waves propagate towards the east, as was also seen in the January 2010 storm during ebb. During low water the peak direction of the with SWAN computed waves is approximately the same as the radar dominant direction: more towards the East, crossing the channel (not shown here).

The radar-SWAN comparisons from Deltares (2010) and Deltares (2014a) give insight in the areas in the Amelander Zeegat where differences in wave direction occur. It is concluded that differences in wave direction are likely in and near the main channel of the Amelander Zeegat.

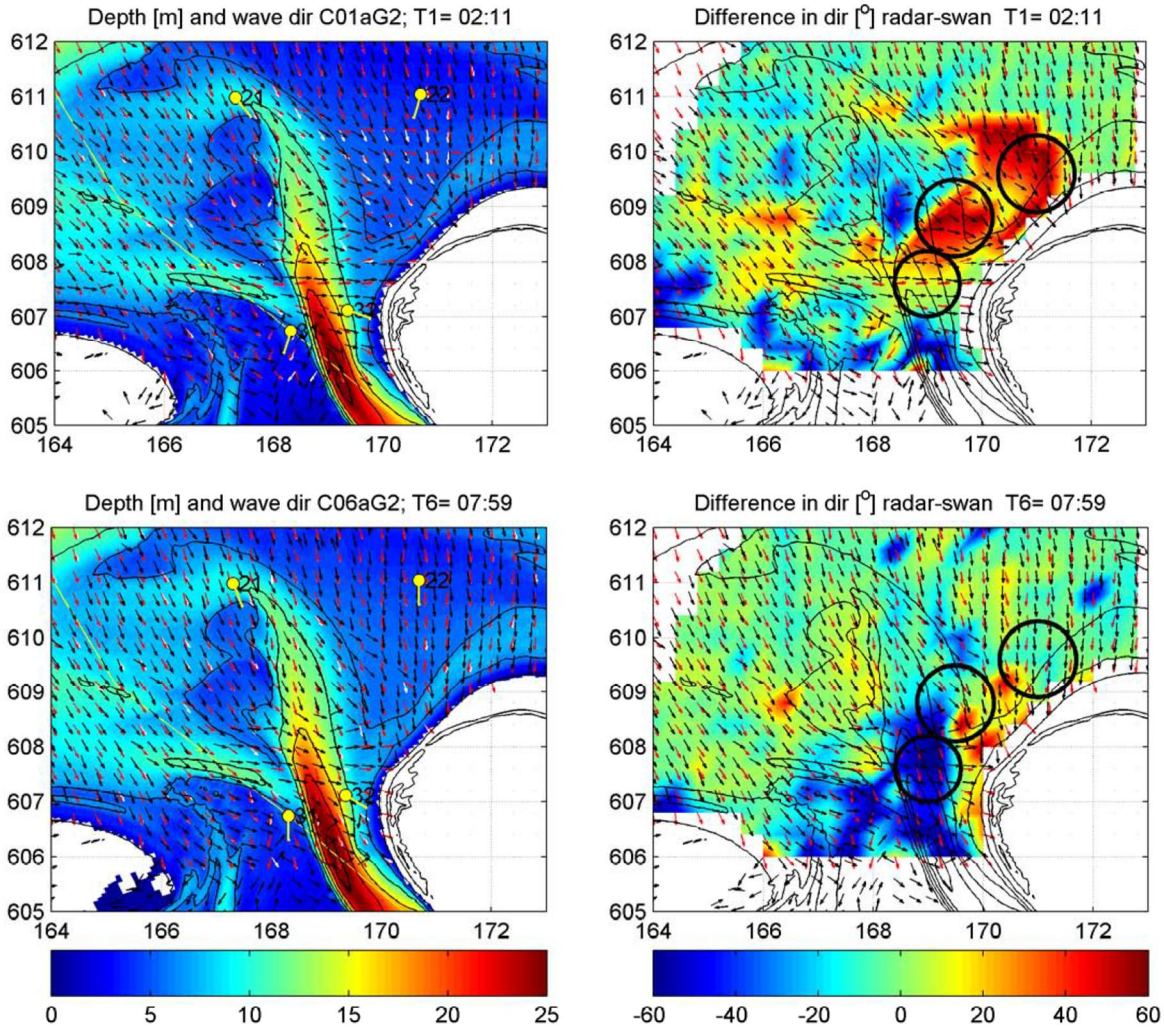

Figure 2.3 Comparison dominant wave direction SWAN and radar as presented in Deltares (2010). Left depth, right difference in dominant direction, vectors: black=radar dominant direction, white=SWAN peak direction and red=SWAN dominant direction.

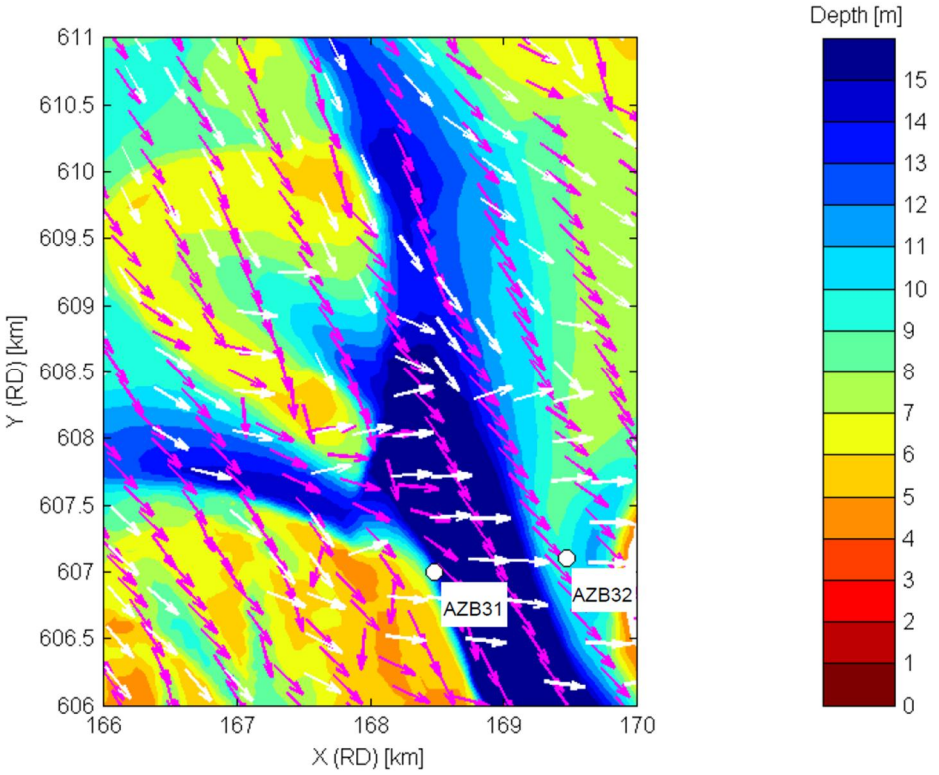

Figure 2.4 Spatial distribution SWAN peak wave directions (pink arrows) and radar dominant wave directions (white arrows) at hindcast moment 5-12-2013 22:00 (HW slack) as presented in Deltares (2014a).

Wave direction and low-frequency wave penetration

In Deltares (2014a) a large number of storms has been analysed to study the penetration of low-frequency energy at different locations inside the Amelander Zeegat. Whether or not the low-frequency energy is underestimated by SWAN depends very much on whether the wave buoy is located close to the tidal channels in the ebb-tidal delta. Near the ebb-tidal delta (for example buoy AZB21), the underestimation of the low-frequency wave height (H_{E10}) is often observed during low water levels. It was seen that the directional spreading of computed directional spectra is smaller than observed for the lower frequencies, and this causes differences when refraction occurs. These conclusions support the findings of Groeneweg et al. (2014a, 2014b).

Groeneweg et al. (2014a, 2014b) showed that two-dimensional nonlinear interactions (and especially the sub-harmonic interactions) play a major role in the transmission of energy from flats into navigation channels, and that this process can explain SWAN's under-prediction of wave energy penetration into a complex tidal inlet system. Sub-harmonic two-dimensional triad interactions play a significant role as they are capable of transferring energy from higher frequencies to lower ones in larger attack angles than the original incident wave input. By their nature, waves created by sub-harmonic waves have broader directionality comparing to the incident waves (Herbers et al, 1995) and thus could provide a mechanism by which energy is transferred over the flat-channel slope. This subharmonic energy transfer is not modelled in SWAN which only includes triad interaction transferring energy to higher harmonics. Furthermore, only wave energy transfer between wave components within the same direction is considered in SWAN, thus a one-dimensional approach.

For buoy AZB31 at the 2013 location large differences can be observed between the measured and computed 2D spectra for hindcast moment 5-12-2013 22:00, see Figure 2.5 (upper panel). The directional spread in the low-frequency energy is larger for the observed spectrum than for the computed spectrum. The measurements show that there is also wave energy propagating from west to east, whereas no wave energy from wave directions smaller than 300 degrees is present in the computed 2D spectra. The radar data in the spatial plot of hindcast moment 5-12-2013 22:00 show that this westerly wave energy comes from the tidal flat west of the channel, see Figure 2.4.

For location AZB32, the 2D spectral plots make clear that SWAN severely overestimates the energy from northerly directions for most hindcast time instances in the wind sea frequency range, see for example hindcast moment 5-12-2013 22:00 (Figure 2.5 lower panel). For some time instances a clear low-frequency energy peak coming from the North is observed in the 2D spectra, whereas this peak is not observed in the measurements. The observed 2D spectra show that the directional spreading for the lower frequencies is broader than in SWAN.

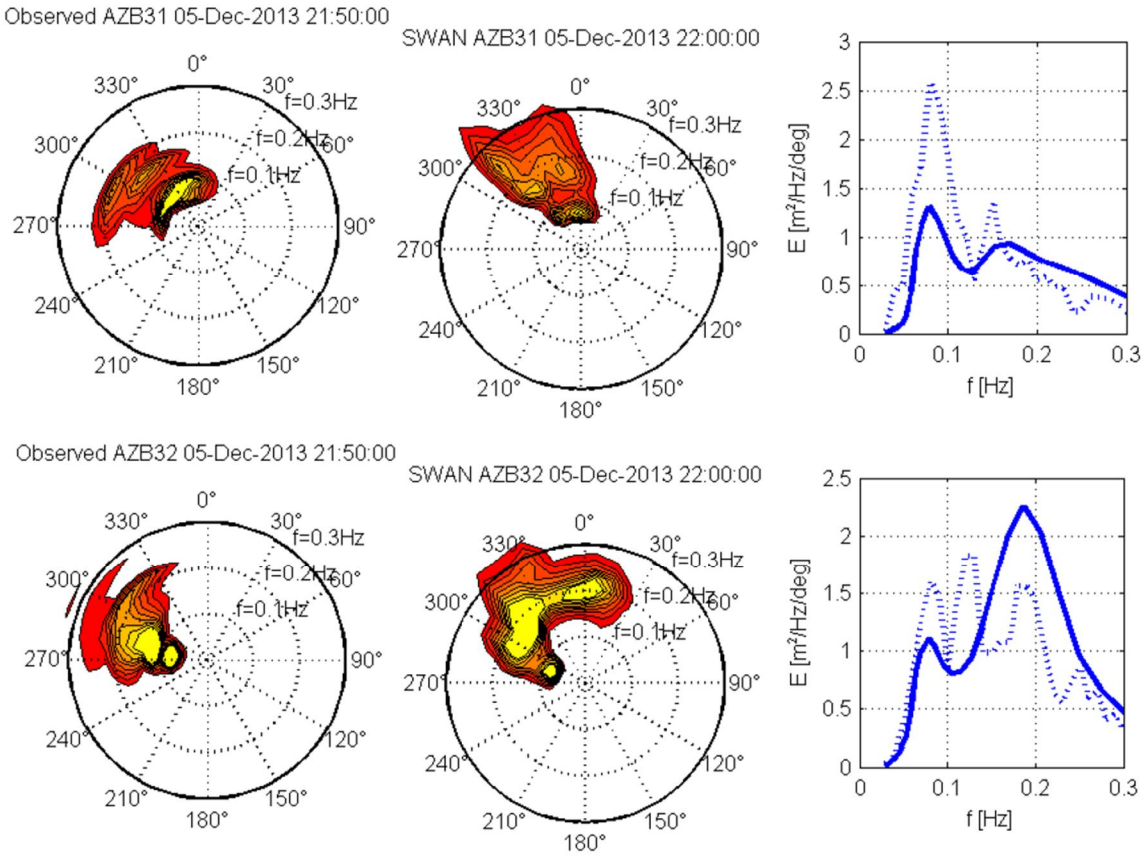

Figure 2.5 2D & 1D wave energy density spectra at AZB31 (upper panel) and AZB32 (lower panel) for hindcast moment 5-12-2013 22:00; first column shows the observed 2D spectrum, the second column the SWAN 2D spectrum and third column the 1D spectrum comparison (SWAN solid line, observed dashed line).

Wave direction and currents/physics

Currents can also influence the mean wave direction. In Deltares (2014b) for instance it was shown that the waves are pushed from a northeasterly direction towards a northerly direction by the current at AZB32, see Figure 2.6, extracted from Deltares (2014b). The red line represents the computation with currents, compared to the blue line representing the

directional spectrum with de-activated currents and the black line the observed directional spectrum.

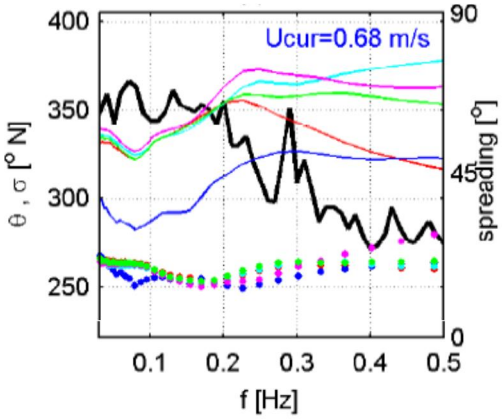

Figure 2.6 Directional wave spectrum 6-12-2013 15:00 (ebb) at AZB32 as presented in Deltares (2014b). Solid lines show the wave direction, dots the directional spreading as function of the frequency. The red line represents the computation with currents, compared to the blue line representing the directional spectrum with de-activated currents and the black line the observed directional spectrum. The other lines represent other variations of the sensitivity study (see Deltares 2014b).

In addition, Deltares (2014b) shows that there are large variations in mean wave direction when the physical settings (whitecapping, enhanced whitecapping due to currents, wind growth) are changed, see the wave direction over the transect from AZB11 to AZB62 in Figure 2.7 for hindcast moment 5-12-2013 22:00. At this hindcast moment series B without currents performs best. The spatial variation in the B-series is least. In this case, it can be said that when currents are neglected the estimation of mean wave direction is better. Further off the coast, the other series all have a mean direction coming more from NNW instead of NW, with the D-series most extremely off. The difference in direction for the D-series reaches up to 60°. On the other hand, the largest difference shown by the B-series with respect to the measured direction is about 20°, and it occurs near AZB31 where a lot of wave refraction occurs due to the complex bathymetry at the entrance of the tidal inlet. However, this does not mean that no current information should be included. It could be that the results in Figure 2.7 are caused by another physical process that is not modelled correctly/ or is absent in SWAN.

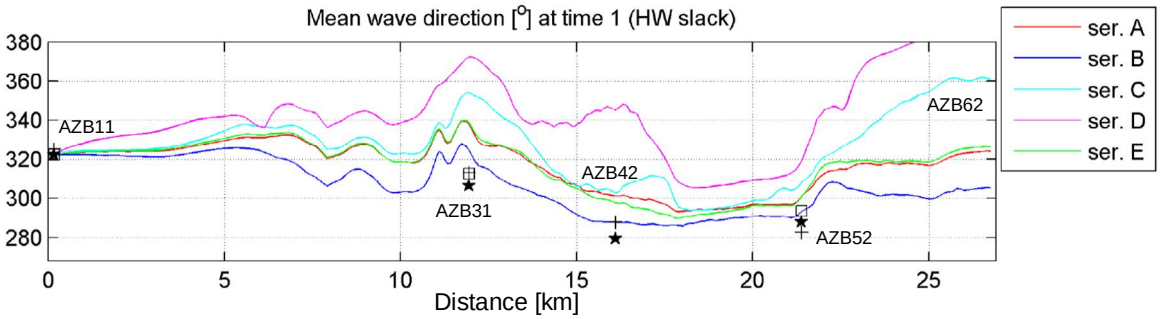

Figure 2.7 Mean wave direction over the transect North Sea AZB11 – over the ebb-tidal delta – towards AZB62 for different SWAN settings at 5-12-2013 22:00. In series A the WTI settings were used, in series B no current was used and in series C, D and E the settings for the whitecapping and/or wind growth settings were changed. Stars indicate observations at the measurement locations (see Deltares 2014b).

Convergence
In Deltares (2014b) the convergence of the mean wave direction has been studied at the measurement locations in the Amelander Zeegat. It was noted that the convergence of wave direction is much slower than the significant wave height or mean wave period. For the locations situated in shallower areas, the wave direction was not fully converged even after 120 iterations.

2.3 Eastern Wadden Sea hindcasts

2.3.1 Hindcasts

Two hindcast studies have been carried out for this area: the November 2007 storm by Alkyon (2008) and the December 2013 storm by Deltares (2014b). Table 2.3 shows the time instances that were hindcasted, with a summary of the conditions during these time instances. The hindcast time instances for the November 2007 storm are instances from the SWIVT database (SWAN Instrument for Validation and Testing, Wenneker et al. 2009) and have been computed by Deltares (2011) with the WTI settings. The December 2013 hindcast has also been done with the WTI settings, but without the Ursell limiter.

	Hindcast time instance	U_{10} (m/s) mean over domain	Udir (°N) mean over domain	Water level (m + NAP) at WEO1	umax (m/s) in the inlet main channel
1	08/11/2007, 19:20	13.1	319	1.3	0.7
2	09/11/2007, 06:20	17.3	326	1.9	0.7
3	09/11/2007, 07:00	19.9	326	2.3	0.8
4	09/11/2007, 07:20	19.4	327	2.5	0.7
5	09/11/2007, 09:00	18.2	332	3.1	0.3
6	09/11/2007, 09:10	18.3	332	3.1	0.2
7	09/11/2007, 09:30	18.4	332	3.1	0.2
8	09/11/2007, 09:40	18.4	332	3.1	0.2
9	09/11/2007, 10:20	18.7	332	3.0	0.3
10	09/11/2007, 11:00	18.9	333	2.8	0.5
11	09/11/2007, 13:40	19.5	333	1.3	1.1
12	05/12/2013, 20:00	19.3	295	1.9	1.0
13	05/12/2013, 22:00	22.9	322	2.9	0.5
14	06/12/2013, 00:00	24.6	303	3.5	0.3
15	06/12/2013, 04:00	21.3	296	1.6	1.6
16	06/12/2013, 07:00	18.9	307	1.6	0.5
17	06/12/2013, 09:00	20.7	298	2.6	0.9
18	06/12/2013, 12:00	20.3	301	2.4	0.5
19	06/12/2013, 14:00	17.0	318	1.4	1.3

Table 2.3 Wind speed, wind direction, water level and maximum current speed at 19 time instances for which a hindcast is performed for the Eastern Wadden Sea

In the eastern Wadden sea the following locations provide directional observations: Borkum (BRKN1), Westereems West (WEW1), Westereems Oost (WEO1), Ranzelgat Noord (RZGN1), Oude Westereems Noord (OWEN), Oude Westereems West (OWEZ), Uithuizerwad1 (UHW1, no data at 5/6 Dec 2013), Lauwers Oost (LAUO1), Boschgat Zuid (BOSZ1), Pieterburenwad (PBW1, no data at 5/6 Dec 2013), Wierumerwad (WRW1, no data at 5/6 Dec 2013) and Schiermonnikoog Westgat (SMWG). The location UHW1, PBW1 and

WRW1 give an idea how well SWAN performs at locations close to the coast. Locations OWEN and OWEZ are not included in the statistical analysis because of less reliable modelled bathymetry due to large morphological changes. These locations were also omitted in the statistical analysis of Deltares (2014b).

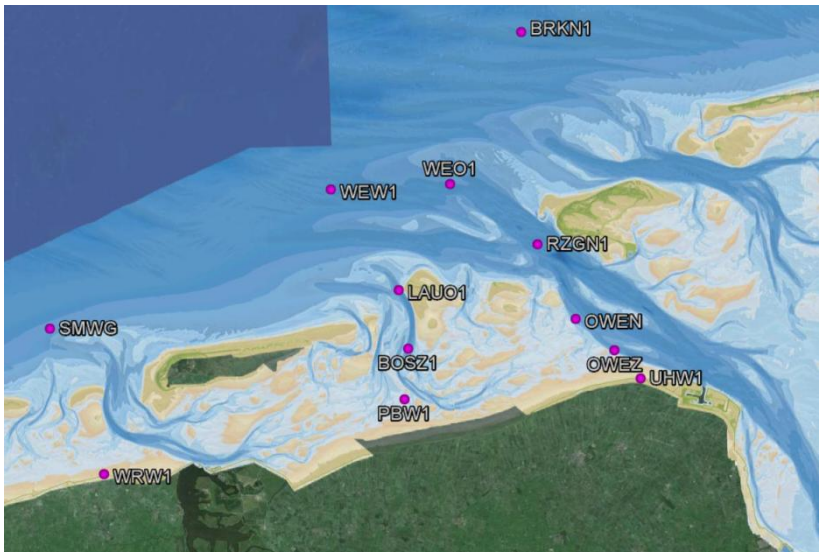

Figure 2.8 Wave measurement locations in the Eastern Wadden Sea.

2.3.2 Statistical comparison

For all wave hindcast time instances presented in Table 2.3, statistics of the wave directions compared to the wave measurements have been calculated, see Table 2.4.

With a bias of 8 degrees and a standard deviation of 5 degrees the wave direction corresponds roughly the same to the measurements as in the Amelander Zeegat. Like in the Amelander Zeegat, the wave direction is in SWAN in most cases more northerly than observed, whereas the directional spreading in SWAN is smaller than observed.

Of the two storms that were hindcasted, the directional parameters of the westerly December 2013 storm are best predicted by SWAN. For the November 2007 a slightly larger bias and standard deviation in the wave direction is seen. The directional spreading is for both storms underestimated by SWAN, with a larger underestimation for the November 2007 storm (-10 degrees) than the December 2013 storm (-5 degrees).

When looking at the directional statistics for each location it can be seen that the computed wave directions of the locations on the North Sea side of the ebb tidal delta compare well with the observed wave directions. The statistics in the channels of RZGN1 are less good, with a bias of almost 16 degrees and a standard deviation of 8 degrees. Apparently, this problem does not occur in the Boschegat (LAUO1 and BOSZ1), as the computed directional parameters compare very well to the observations.

Finally, a bias in mean wave direction is seen of 9-18 degrees between SWAN and the observation at the locations near the coast (UHW1, PBW1 and WRW1) and the directional spreading is underestimated by 10-20 degrees. The bias at the buoys UHW1 and WRW1 is significantly higher (18^o and 16^o respectively) than the bias in PBW1 or in AZB52. From the measurements, presented in Alkyon (2008) it is seen that the low-frequency wave penetration at locations UHW1 and WRW1 is significant. As SWAN has some difficulties to predict the

low-frequency wave penetration, it is more likely that larger errors occur in mixed swell and wind-sea sea states.

	Wave direction					Directional spreading					
	Bias [°]	**stdev [°]**	**Rmse [°]**	**X_{mean} [°]**	**Y_{mean} [°]**	**Bias [°]**	**stdev [°]**	**Rmse [°]**	**X_{mean} [°]**	**Y_{mean} [°]**	**N**
All	7.96	4.85	12.8	316	324	-6.94	5.65	9.36	34	27	86
Nov 2007	9.74	5.3	14.37	320	330	-10.3	6.05	12.46	38	28	32
Dec 2013	7.02	4.67	11.7	313	320	-4.95	4.43	6.9	32	27	54
BRKN1	1.92	1.73	2.59	320	322	0.23	0.77	0.8	28	29	8
WEW1	6.94	3.2	7.65	322	329	-3.35	5.71	6.63	26	23	8
WEO1	6.53	6.34	12.31	307	314	-2.91	2.98	4.18	36	33	19
RZGN1	15.89	7.75	17.89	298	314	-9.07	3.83	9.85	34	24	8
UHW1	**17.62**	**5.91**	**19.38**	**331**	**348**	**-18.6**	**3.2**	**18.9**	**42**	**24**	**7**
LAUO1	6.68	4.25	8.04	301	308	-6.7	3.01	7.35	35	28	8
BOSZ1	1.26	8.41	12.02	318	320	-4.84	2.54	5.47	34	29	8
PBW1	**8.75**	**4.25**	**9.79**	**332**	**340**	**-10.8**	**1.17**	**10.9**	**41**	**30**	**5**
SMWG	-1.72	6.12	7.6	333	331	-7.23	5.99	9.77	27	19	6
WRW1	**16.09**	**6.38**	**18.11**	**319**	**335**	**-13.7**	**2.48**	**14.0**	**39**	**25**	**9**

Table 2.4 Statistics for wave direction and directional spreading for the Eastern Wadden Sea. The locations closest to the coast are made bold.

2.3.3 Findings with respect to SWAN wave directions at the Eastern Wadden Sea

In this section, findings from existing studies with respect to SWAN wave directions are summarized. The findings of the two hindasts are considered; the November 2007 storm and the December 2013 storm. In this section the focus has been on the areas where problems with the prediction of the wave direction were identified. Here these problems are briefly summarized with some examples from the hindcast studies. In the existing hindcast studies these problems have been illustrated in more detail/ with more examples.

November 2007 storm

During the November 2007 storm, directional measurements were done close to the mainland dikes (WRW1, UHW1). The measured spectra at these buoy locations clearly show that low-frequency waves can penetrate into the Wadden Sea and up to the mainland dikes. On the other hand it was found by Alkyon (2008) that SWAN generally underestimates the penetration of the low-frequency wave components, see e.g. hindcast moment 09-11-2007 9:40 in Figure 2.9. An exception occurs for the moment with the highest water level (not shown here, see Alkyon 2008). Local wind seas are better predicted by SWAN than the low-frequency waves. This is also seen in the mean wave direction in Figure 2.9, where the difference in mean wave direction and directional spreading is largest for frequencies smaller than 0.2 Hz.

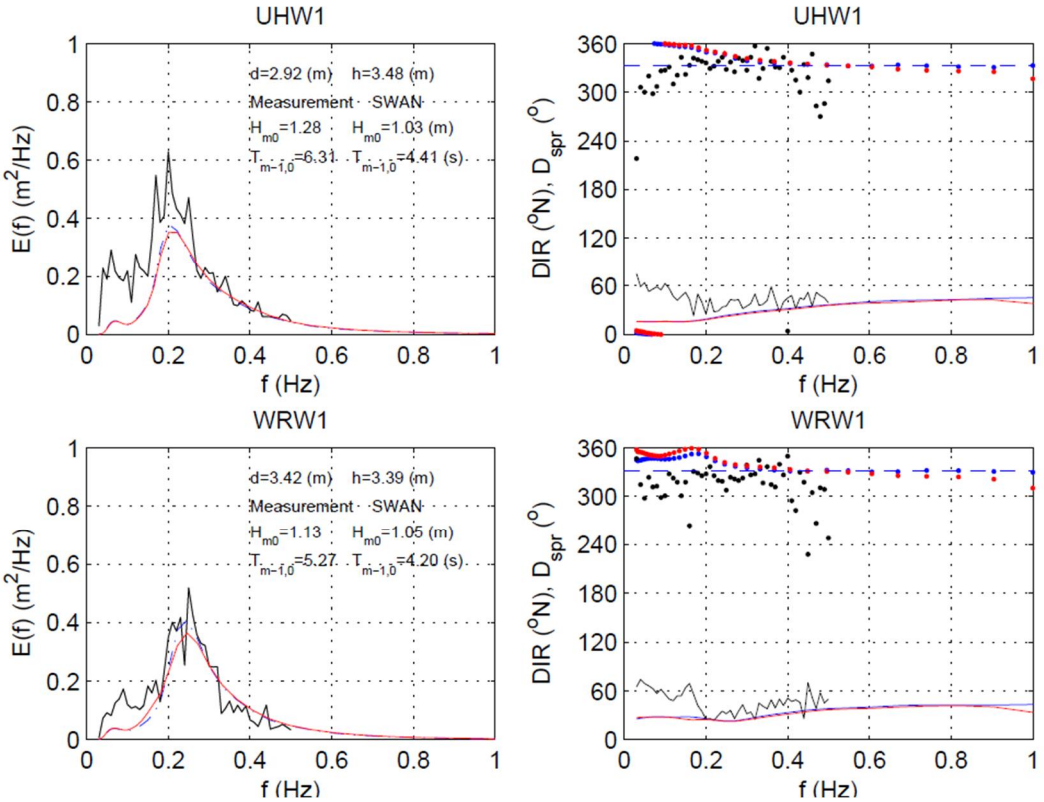

Figure 2.9 Comparison measured and computed spectra UHW1 and WRW1, variation of mean wave direction and directional spreading, wind direction (blue dashed line) for hindcast moment 09-11-2007 9:40. Measurements are shown in black, SWAN in red and SWAN with the current deactivated in blue. As presented in Alkyon (2008).

December 2013 storm

In Deltares (2014a) the low-frequency wave penetration was studied during the December 2013 storm comparing computed 2D spectra to observed 2D spectra. For this north-westerly storm, a large part of wave energy computed by SWAN crosses the ebb-tidal delta and then enters the channel from a north to north-westerly direction. The 2D wave spectra of the December 2013 storm showed that the directional wave energy distribution at the wave buoys is often different in the observed spectra than in SWAN. Some of the differences in directional wave distribution between the measured and computed wave energy can be directly related to features in the geometry and the resulting effect of nonlinear wave interactions (as explained in Section 2.2.3). As a consequence, wave energy enters the channel from a different direction than modeled in SWAN. For example, the low-frequency wave energy that propagates over the tidal flat west of RZGN1 is able to reach RZGN1 in the measurements and not in the SWAN computations, see Figure 2.10.

Figure 2.10 shows that the wave energy peak for SWAN is at ca. 305 degrees, whereas the observed wave energy peak is at ca. 290 degrees. This means that the main part of the wave energy in SWAN comes from the channel (and crossed the ebb-tidal channel to the north/northwest of RZGN1 before). As the wave direction is parallel to the channel, the energy propagates through the channel. However, the measured peak direction shows that most energy comes from the shallow flat northwest of RZGN1.

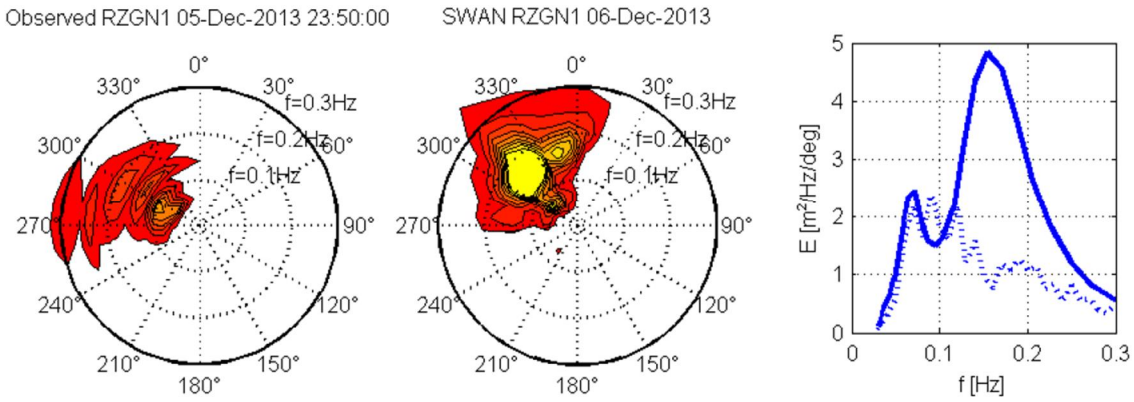

Figure 2.10 2D & 1D wave energy density spectra at RZGN1 for hindcast moment 6-12-2013 00:00; first column shows the observed 2D spectrum, the second column the SWAN 2D spectrum and third column the 1D spectrum comparison (SWAN solid line, observed dashed line). As presented in Deltares (2014a).

2.4 Western Scheldt hindcasts

2.4.1 Hindcasts

For the Western Scheldt, SWAN hindcasts of six different storms at 30 different time instances were performed, all by Witteveen+Bos (2010). Table 2.5 gives an overview of all hindcast time instances, including information on the wind velocity, wind direction and water level during those time instances. All hindcast computations have been done with the WTI settings. In the Western Scheldt the wave directions are only measured at Deurlo (DELO) and Cadzand (CADW), see Figure 2.11.

	Hindcast time instance	U_{10} (m/s) mean over domain	Udir (°N) mean over domain	Water level (m NAP) at station WIEL
1	26/10/02, 02:00	18.69	257	1.55
2	27/10/02, 18:00	22.59	283	2.42
3	27/10/02, 19:30	20.12	288	1.92
4	20/12/03, 21:30	15.59	242	1.27
5	21/12/03, 06:30	18.18	256	-0.52
6	21/12/03, 08:00	18.61	268	0.16
7	21/12/03, 15:00	14.46	297	1.57
8	07/02/04, 01:00	14.86	241	1.36
9	07/02/04, 10:00	15.03	258	-1.00
10	08/02/04, 06:00	20.23	269	1.07
11	08/02/04, 07:00	21.11	276	0.36
12	08/02/04, 16:30	18.19	315	2.87
13	08/02/04, 18:00	18.07	317	1.96
14	12/02/05, 08:30	18.26	235	-0.93
15	12/02/05, 10:30	18.36	239	-2.08
16	13/02/05, 06:00	15.56	278	2.58
17	13/02/05, 08:30	15.45	283	0.33
18	14/02/05, 00:00	17.32	340	-0.47
19	14/02/05, 08:30	13.28	331	0.56
20	14/02/05, 13:30	14.94	318	-0.88
21	09/11/07, 01:30	16.49	327	3.45
22	09/11/07, 04:30	15.97	326	1.96
23	09/11/07, 07:30	18.64	322	0.73
24	09/11/07, 10:00	16.71	320	1.21
25	09/11/07, 14:00	14.98	326	2.97
26	09/11/07, 17:00	14.38	310	0.56
27	29/02/08, 22:30	18.88	235	-0.19
28	29/02/08, 23:30	19.31	238	-0.67
29	01/03/08, 03:30	19.85	247	0.06
30	01/03/08, 06:00	19.60	288	2.01

Table 2.5 Wind speed, wind direction and water level at 30 time instances for which a hindcast is performed for the Western Scheldt estuary, see also Witteveen+Bos (2010).

Figure 2.11 Wave measurement locations in the Western Scheldt. The directional wave measurement locations are shown with magenta dots.

2.4.2 Statistical comparison

For all wave hindcast time instances presented in Table 2.5, statistics of the wave directions compared to the wave measurements have been calculated, see Table 2.6.

With a bias of almost zero and a standard deviation of 3 to 4 degrees, the overall agreement between the directional parameters of SWAN and the measured directional parameters can be considered very good.

For two of the storms SWAN predicts a more northerly direction, whereas for three storms the computed wave direction is more southerly than observed. However, the biases are for all storms less than 5 degrees and almost no bias in the directional spreading is observed. Finally, both locations show a very good comparison between computed and measured directional parameters.

It must be noted that the locations with directional observations are located in the relatively open mouth of the Western Scheldt. Larger directional differences are expected inside the Western Scheldt, but due to the lack of directional measurements, they have not been considered in this study.

	Wave direction					Directional spreading					
	Bias [°]	**stdev [°]**	**Rmse [°]**	**X_{mean} [°]**	**Y_{mean} [°]**	**Bias [°]**	**stdev [°]**	**Rmse [°]**	**X_{mean} [°]**	**Y_{mean} [°]**	**N**
All	0.03	3.91	4.61	297	297	-0.63	2.94	3.09	27	26	50
Oct 2002	0.52	3.92	4.2	292	293	-1.46	1.57	2.15	27	26	6
Dec 2003	-1.25	3.46	3.71	289	288	-1.08	3.73	3.95	28	27	8
Feb 2004	2.61	4.17	5.35	294	297	-0.79	3.2	3.34	27	27	12
Feb 2005	0.04	4.18	4.22	303	303	-0.66	2.96	3.15	28	27	14
Nov 2007	-1.35	1.3	1.87	324	323	-0.86	0.38	0.94	25	24	6
Mar 2008	-4.18	6.39	7.63	270	266	2.52	2.36	3.45	22	25	4
DELO	-0.34	2.7	2.74	300	300	0.17	1.58	1.59	24	25	28
CADW	**0.4**	**5.33**	**6.23**	**294**	**294**	**-1.64**	**3.94**	**4.31**	**30**	**29**	**22**

Table 2.6 Statistics for wave direction and directional spreading for the Western Scheldt. The location closest to the coast is made bold.

2.5 Conclusions existing hindcasts Amelander Zeegat, Eastern Wadden and Western Scheldt

- In most Wadden Sea cases SWAN predicts a more northerly mean wave direction and underestimates the directional spreading (on average 5-10 degrees bias in mean wave direction and directional spreading in the Wadden Sea).
- SWAN predicts the mean wave direction and directional spreading well in the outer (offshore) measurement locations (e.g. see AZB11, AZB12 and BRKN1).
- The differences between observed and computed wave directions are largest in the tidal channels. In Deltares (2014a) this was related to the fact that SWAN does not model the sub-harmonic nonlinear interactions that broaden the directional spectrum. Therefore, the waves refract differently, when encountering tidal channels. In addition, currents play a role, as was shown in Deltares (2014b). These factors can explain the more northerly mean wave direction and the smaller directional spreading in SWAN.
- There are limited directional measurements available close to the coast. However, the few observations show that biases between SWAN and observations of 10 to 20 degrees in the mean wave direction are likely with a standard deviation of circa 5 degrees. In addition, the directional spreading is underestimated by SWAN with 10 to 20 degrees and the standard deviation is a few degrees.
- The wave direction along the coast, especially in the Amelander Zeegat, is predominantly influenced by locally generated wind waves, yielding mean wave directions that are more or less equal to the wind direction.
- The agreement between the computed and measured mean wave directions is better in cases where wind-sea predominates than in cases where low-frequency wave penetration is measured.

3 Sensitivity of the hydraulic load function and required crest heights to nearshore wave direction

3.1 Introduction

The quality of the nearshore wave directions of SWAN is important for the estimation of required crest heights and the hydraulic loads for the following reasons:

- The wave angle with respect to the dike orientation is taken into account in the run-up and overtopping calculations to calculate the required crest height of the water defences. In Section 3.2 it is assessed how sensitive the required crest height is to variances in the wave direction.
- In assessing the stability of revetments a load function is used. This function is influenced by the wave direction. In Section 3.3 the sensitivity of the load function to bi-modal sea states is presented.

The conclusions and recommendations of the analyses of Section 3.2 and 3.3 have been presented in Section 3.4.

3.2 Influence wave direction on required crest height water defence

3.2.1 Formulations to determine the crest height

The required crest height as determined by Hydra-K is based on the wave run-up and wave overtopping formulas. The formulations for wave run-up and overtopping do include wave direction, using the coefficient γ_β which could – more or less – be considered as a reduction factor on the significant wave height H_{m0}. The 'Technisch Rapport Golfoploop en Golfoverslag bij Dijken' (TAW; May 2002) indicates that the coefficient γ_β for wave overtopping is depending on the angle of wave attack relative to the dike normal (β) as follows:

$\gamma_\beta = 1 - 0.0033 * \beta$ for $0^o \leq |\beta| \leq 80^o$ (β=0: normal wave incidence)
$\gamma_\beta = 1 - 0.0033 * 80$ for $|\beta| > 80^o$

The angle of wave attack (β) is the difference between the wave direction and the dike normal.

The formula for wave run-up is rather similar, but has a value of 0.0022 instead of 0.0033. Figure 3.1 shows coefficient γ_β as a function of the angle of wave attack relative to the dike normal for run-up and overtopping.

In cases where the angle of wave attack is larger than 80^o but smaller than 110^o, the coefficient γ_β stays constant and an additional correction on the wave height H_{m0} and wave period $T_{m-1,0}$ is advised by TAW (2002) for wave overtopping and wave run-up:

- H_{m0} is multiplied by a factor $\frac{110-|\beta|}{30}$
- $T_{m-1,0}$ is multiplied by a factor $\sqrt{\frac{110-|\beta|}{30}}$

For angles of wave attack $110^o < |\beta| \leq 180^o$ H_{m0} is zero.

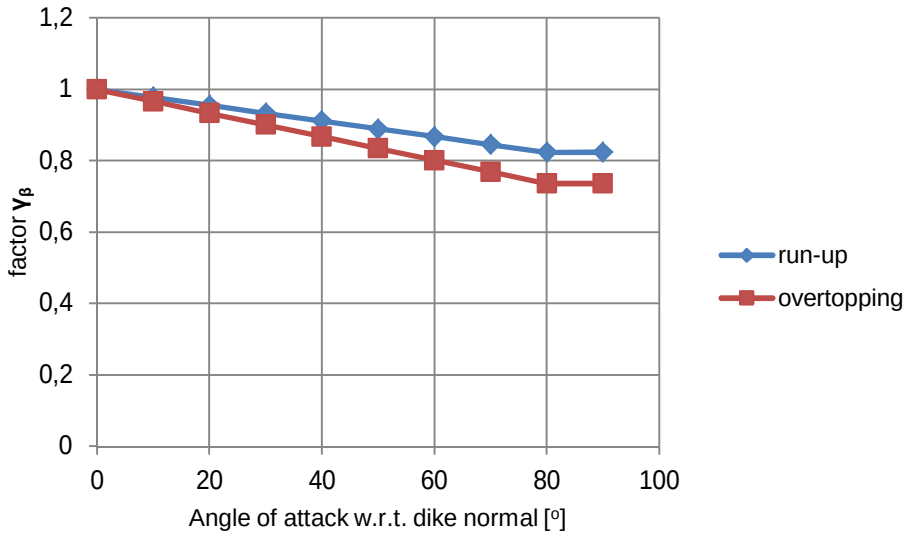

Figure 3.1 Coefficient γ_β as a function of the angle of attack with respect to the dike normal for run-up (blue line) and overtopping (red line).

3.2.2 Sensitivity analysis crest height

The required crest height of a water defence is not only depending on H_{m0} and γ_β, but also – among other things – on the overtopping discharge, slope angle and whether waves are breaking or not. Therefore, the influence of the wave direction will not be the same for all locations.

To get an idea of the influence of the wave height on the required crest height, a sensitivity analysis was performed on the wave overtopping calculations in Hydra-K, using the CR-2011 database. For this sensitivity analysis three locations in the Wadden Sea were chosen, see Figure 3.2. To study the effect of a more southerly or northerly wave direction on the crest height, the wave directions in the CR-2011 database at these locations were changed by -20°, -10°, 10° and 20°. These values were chosen, as these are likely errors, according to Section 2.5, for nearshore locations. Hydra-K default cross sections were used for this calculation. The details of the three locations are shown in Table 3.1. Locations 1 and 2 have an angle of wave attack larger than 60 degrees with respect to the dike normal.

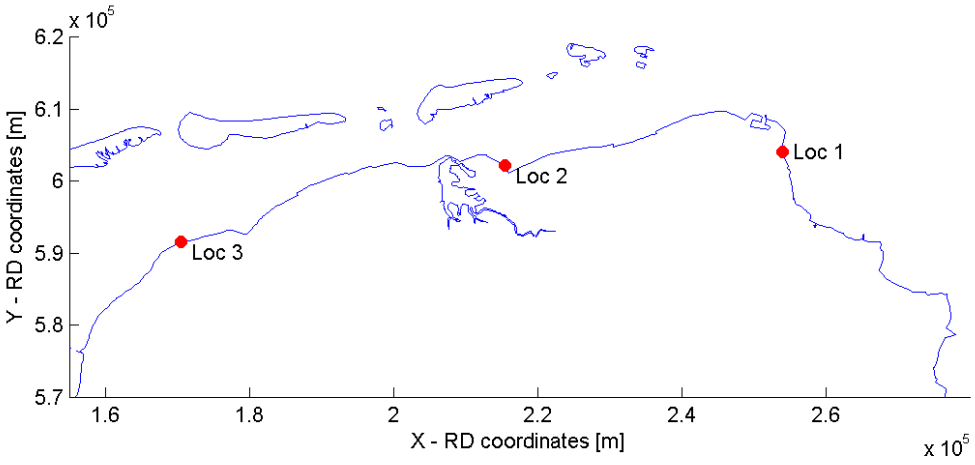

Figure 3.2 Locations for sensitivity analysis

on	Area	Hydra-K location	X RD [m]	Y RD [m]	Orientation coast [°N]	Wave direction [°N]	Angle of wave attack β [°]
Loc 1	Eems-Dollard	10871	253966	604083	92	27	65
Loc 2	Lauwersoog	10659	215402	602178	39	330	69
Loc 3	Amelander Zeegat	10432	170459	591574	357	317	40

Table 3.1 Details locations for sensitivity analysis

Figure 3.3 shows the results of the sensitivity analysis. The black dots show the crest height for the reference run with the original angle of wave attack. The effect of the variations of -20, -10, +10 and +20 degrees in wave direction are shown for the three locations. Due to the fact that each marker represents a probabilistic calculation (an illustration point is calculated for which the crest height is normative) and certain conditions could become more dominant with a different wave direction, the angle of attack with respect to the dike normal can be larger or smaller than the 10 or 20 degrees variation.

For angles of attack smaller than circa 75 degrees the crest height changes by circa 7-10 centimetres for a 10° difference in wave direction. However, for angles of wave attack larger than circa 75 degrees the influence of the wave direction on the crest height is much larger. Location 1 and 2 show a difference of circa 30 centimetres in crest height for a 10° difference in wave direction when the angle of attack is larger than circa 75 degrees. This can be related to the correction on the wave parameters H_{m0} and $T_{m-1,0}$, that is used when the angle of wave attack relative to the dike normal is more than 80 degrees, but smaller than 110 degrees.

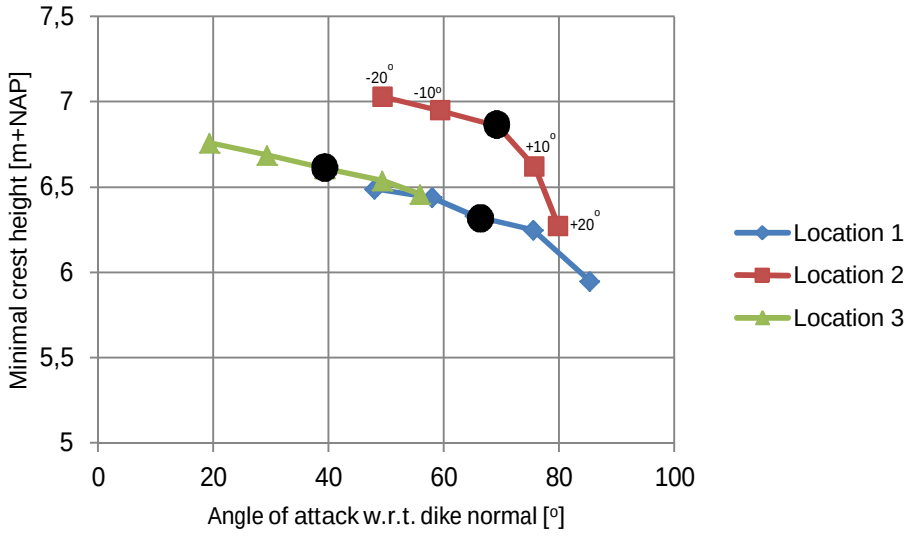

Figure 3.3 Sensitivity analysis angle of wave attack relative to dike normal for three locations. Variations of -20, -10, +10 and +20 degrees relative to the wave direction have been considered. The black dots show the reference run, with the original angle of wave attack.

This sensitivity analysis gives an idea of the differences in crest height that could be the result of a 10° or 20° error in the wave direction. The influence of an error in the wave direction is the largest in case of waves with an angle of attack relative to the dike normal of more than 75-80 degrees. This can be expected, taking into account that the crest height formula in

section 3.2.1 also changes at 80 degrees and the H_{m0} and T_{m-10} are multiplied with a factor for $80^o < |\beta| \leq 110^o$.

3.2.3 Areas with wave attack angles larger than 75°

In the previous section it was concluded that the required crest height is more sensitive to differences (e.g. errors) in wave direction when the angle of wave attack is larger than ca. 75 degrees. In order to identify the areas in the Wadden Sea and the Western Scheldt where the angle of wave attack is larger than 75°, the Hydra-K results for WTI2011 (in the illustration point) with respect to the required crest height have been analysed.

Figure 3.4, shows the wave direction at the Hydra-K output locations in the Wadden Sea. The red arrows indicate waves that are more than 75° off the dike normal. At the southern side of the islands of Ameland and Schiermonnikoog as well as in the Eems Dollard, the dominant wave attack at the dike is often from a large angle of wave attack. In the remaining areas the coastal orientation is roughly perpendicular to the storm direction (north to north-westerly storms) or refraction turns the waves and therefore decreases the angle of wave attack.

Figure 3.5 shows the wave direction at the Hydra-K output locations for the criterion wave overtopping in the Western Scheldt. It can be seen that the angle of wave attack inside the Western Scheldt is for many locations more than 75°.

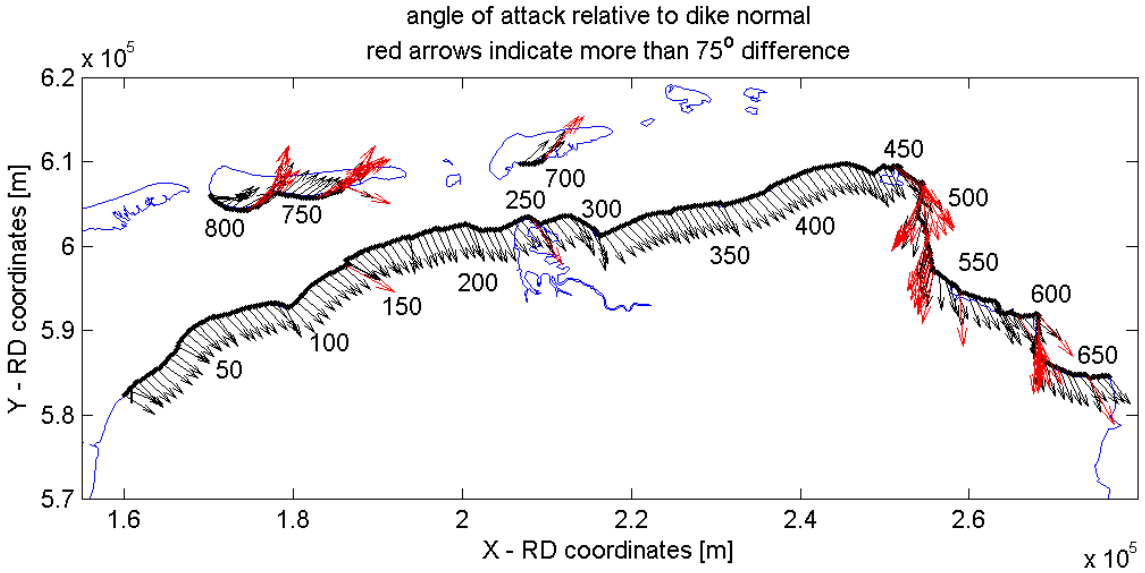

Figure 3.4 Angle of wave attack relative to the dike normal in the Wadden Sea, black arrow (every 4th location is shown) indicate an angle of wave attack smaller than 75°, red arrows indicate an angle of wave attack of more than 75°.

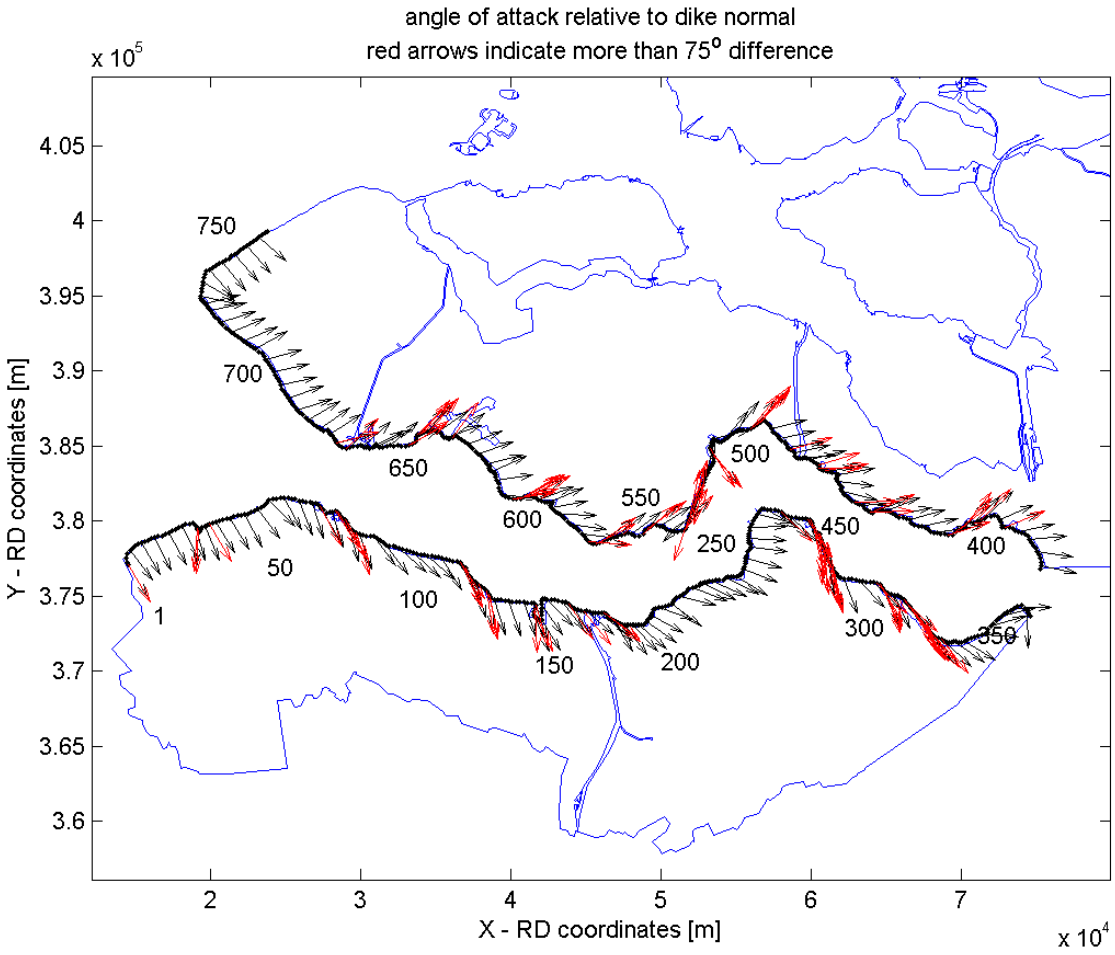

Figure 3.5 Angle of wave attack relative to the dike normal in the Western Scheldt, black arrow (every 4th location is shown) indicate an angle of wave attack smaller than 75°, red arrows indicate an angle of wave attack of more than 75°.

3.3 Sensitivity hydraulic loads to bi-modality

At this moment the representative hydraulic load (B) that is used for a certain failure mechanism (for example the stability of revetments) is determined based on one or more of the integral wave parameters; significant wave height H_{m0}, peak period T_p and mean angle of wave attack relative to the dike normal β. The simplified load function entails:

$$B = H_{m0}^{a} T_p^{b} \cos(\beta)^{c/2}$$

Where a, b en c are known constants.

In this formula it is assumed that the wave energy comes from one direction. However, in some cases, for example when swell and wind-sea are present, the sea-state is bi-modal, which means that the wave energy at one location comes from two different directions. In this section the sensitivity of hydraulic loads to bi-modality is discussed, as was shown in Smale and Wenneker (2011).

To study the sensitivity of hydraulic loads to bi-modality, the simplified load function has been reformulated as a measure of energy E, from two different directions (with the same period):

$$B = \left(4\sqrt{\mathrm{E}_1 \cos(\beta_1)^c + \mathrm{E}_2 \cos(\beta_2)^c} \right)^a T_p^b$$

In this formula β_1 is the primary wave direction and β_2 the secondary wave direction relative to the coast normal, see Figure 3.6.

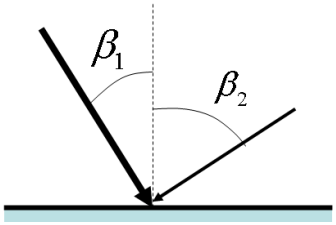

Figure 3.6 Primary and secondary angle of wave attack relative to the coast normal

With these formulas the difference in hydraulic load was determined in case the load was either based on one wave direction or in case it was based on two wave directions, see Figuur 3.7 (as presented in Smale and Wenneker (2011)). In this example $a = b = c = 1$ was used and three different angle differences $\Delta\Theta = |\beta_1 - \beta_2|$ between the primary and the secondary wave direction were used; 30°, 45° and 90°.

In Figuur 3.7 the relative difference in hydraulic load due to the inclusion of a secondary wave direction in the load function is presented. It can be seen that the relative difference in hydraulic load can be large for large angles of wave attack (β_1> 60°). From this analysis it can be concluded that in case of large angles of wave attack and the presence of bi- or multi-modal sea states the hydraulic load could be underestimated. However, it should be noted that this is a very basic analysis and many assumptions and simplifications were made. It is for example very likely that the primary and secondary wave direction do not have the same peak period and that a different assumption of the a, b and c values results in a different relative hydraulic load difference.

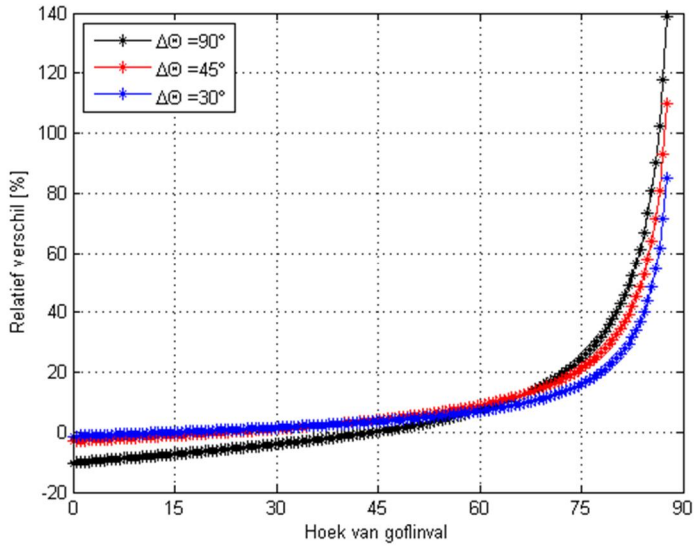

Figuur 3.7 Relative difference in hydraulic load ($B(\beta_1, \beta_2) - B(\beta_1)/B(\beta_1)$) due to the inclusion of a secondary wave direction. Three different angle differences β_1-β_2 were studied; 30°, 45° and 90°. As presented in Smale and Wenneker (2011).

3.4 Conclusions and recommendations

3.4.1 Conclusions on the influence of wave direction on required crest height water defence

- The sensitivity analysis of the wave direction on the required crest height has shown that the effect of an error in the wave direction is largest when the waves are slanting (more than 75^{o}). In these cases an error of 10 degrees in wave direction could result in an error in crest height of 30 centimetres. This value is indicative, as only three locations were considered in the sensitivity analysis.
- In contrast, in cases were the angle of wave attack is less than 75^{o}: an error of 10 degrees in the wave directions results in an error in crest height of 7-10 centimetres. These values are indicative, as only three locations were considered in the sensitivity analysis.
- Locations with an angle of wave attack larger than ca. 75 degrees during normative conditions occur at the southern side of the islands of Ameland and Schiermonnikoog as well as in the Eems Dollard and inside the Western Scheldt.

3.4.2 Conclusions sensitivity hydraulic load to bi-modality

- The hydraulic loads are very sensitive to the inclusion of a secondary wave direction in the load function when the angle of wave attack relative to the dike normal is large (larger than 60^{o}).

3.4.3 Recommendations

- More research is necessary into the effect of bi- or multi modal sea states on the hydraulic loads, as the analysis shown in Section 3.3 was very basic analysis and many assumptions and simplifications were made. In this respect it would be useful to make better use of measured 2D wave spectra, using the measured 2D wave spectra to quantify where and how often bi- or multi modal sea states occur along the Dutch Wadden Sea and Western Scheldt coast. Furthermore, the effect of bi- or multi modal sea states on hydraulic loads could be studied in more detail by studying relevant literature, existing field and laboratory experiments or/and using numerical models.
- In Section 3.2 a sensitivity study was done on the influence of the wave direction on the required crest height of the water defence. This was done for only three locations by changing the angle of wave attack in the Hydra-K database. To confirm the results found in this analysis, a more thorough analysis is recommended by looking at more output locations in Hydra-K.

4 Sensitivity of wave direction to model inputs and physics

4.1 Introduction

In chapter 2 the agreement between modelled and observed wave directions at various locations was studied. However, most measurement locations are not located close to the water defences and it is therefore hard to draw conclusions on the validity of the SWAN wave directions along the coast. Furthermore, the measured storms were severe storms, but not extreme (in the order of 1/4000 year return periods). It is therefore possible that the conclusions on the performance of SWAN are different during extreme events when water levels are high and the low-frequency wave penetration possibly more dominant. To get an idea of the conditions during extreme events the most important conclusions of the sensitivity analysis in the Amelander Zeegat (WL & Alkyon (2007)) regarding wave direction are summarized in Section 4.2. In addition, various extreme events have been studied from the CR-2011 database, including the entire Wadden Sea and the Western Scheldt (see Section 4.3).

4.2 Sensitivity analysis Amelander Zeegat, WL & Alkyon (2007) to model physics and inputs

WL & Alkyon (2007) carried out a sensitivity analysis to determine the effect of variations in model physics and model inputs on the wave conditions at the primary sea defences along the Frisian and Ameland coasts. In this regard, a selection of observed severe storms (NW) as well as hypothetical extreme events (NW and SW) was considered. The investigated sensitivities included: sensitivity to offshore boundary conditions, the effect of currents, sensitivity of wind speed, wind direction and spatial variation in the wind field, the effect of water level on low-frequency waves and sensitivities to shallow water source terms.

Boundary conditions

A significant finding of this study is that the wave conditions at the Frisian coast (south of the Amelander Zeegat) are not very sensitive to wave conditions imposed at the North Sea boundary, even during extreme NW storm events. In this regard, the outer delta of the tidal inlet works as a filter that blocks most of the waves coming from the North Sea. Variations of 10% in the significant wave height and period, and 10^{o} in the mean direction and directional spreading at the boundary leads to changes of only up to 0.02% in the significant wave height, mean period and directional spreading, and up to 0.02^{o} in the mean direction. Figure 4.1 shows the differences in mean wave direction when the mean wave direction at the outer boundary is changed with 10^{o} during an extreme north-westerly storm. It can be seen that the tidal inlet of Ameland is not affected by changes in wave direction in the offshore boundary. This insensitivity is due to the saturated conditions that exist in the surf zone on the ebb tidal delta, in which wave energy is significantly dissipated.

Water level

The ebb tidal delta dissipates a substantial amount of wave energy arriving from the North Sea. The degree to which wave energy is dissipated is determined for a large part by the water depth (bathymetry and water level). In the case that the water level of the extreme NW storm was increased by 1 m (to +5.7 m+NAP), wave heights and mean periods were found to increase by 24% and 15% respectively. The increase in the values of these parameters is due to the higher asymptote value of the shallow water wave growth limit, and the fact that the saturated conditions along the foreshore allow a higher wave height at the primary sea defence, see Figure 4.2 for an example of the differences that were seen in the wave spectra

near the coast. The mean wave direction and directional spreading did not change significantly in this case, see Figure 4.3 for the change in mean wave direction.

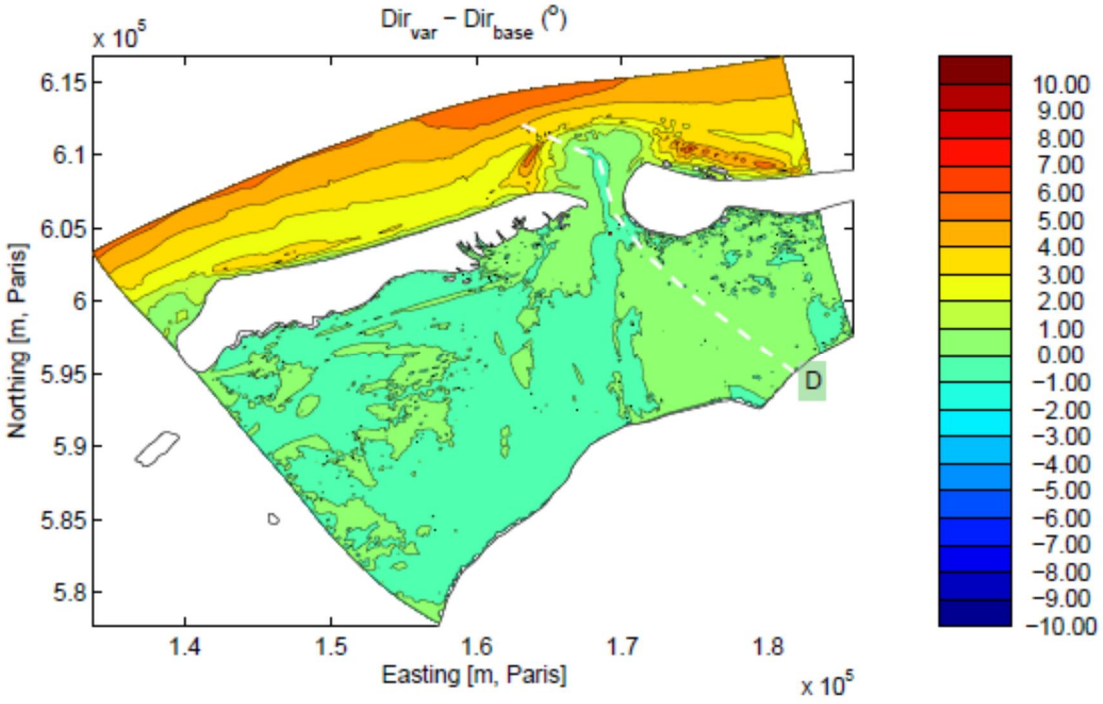

Figure 4.1 Differences in mean wave direction for a +10^o variation in wave direction at the North Sea boundary (outer domain, not shown) during an extreme NW storm (wind direction = 315^o, U_{10} = 34 m/s, water level = 4.7 m+NAP, $H_{m0\_boundary}$ = 9,4 m, $T_{p\_boundary}$ = 18 s). As presented in WL&Alkyon (2007).

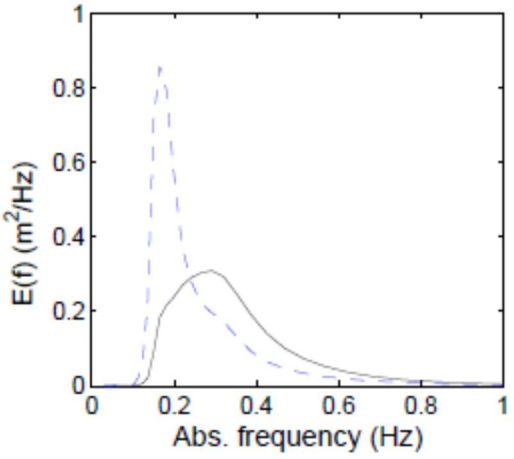

Figure 4.2 Differences in wave spectra close to the coast (curve D in Figure 4.3) for an increase in water level of 1 m during an extreme NW storm (wind direction = 315^o, U_{10} = 34 m/s, water level = 5.7 m+NAP, $H_{m0\_boundary}$ = 9,4 m, $T_{p\_boundary}$ = 18 s) The base run is shown as a solid black line, the variation is shown with a blue dashed line. As presented in WL & Alkyon (2007).

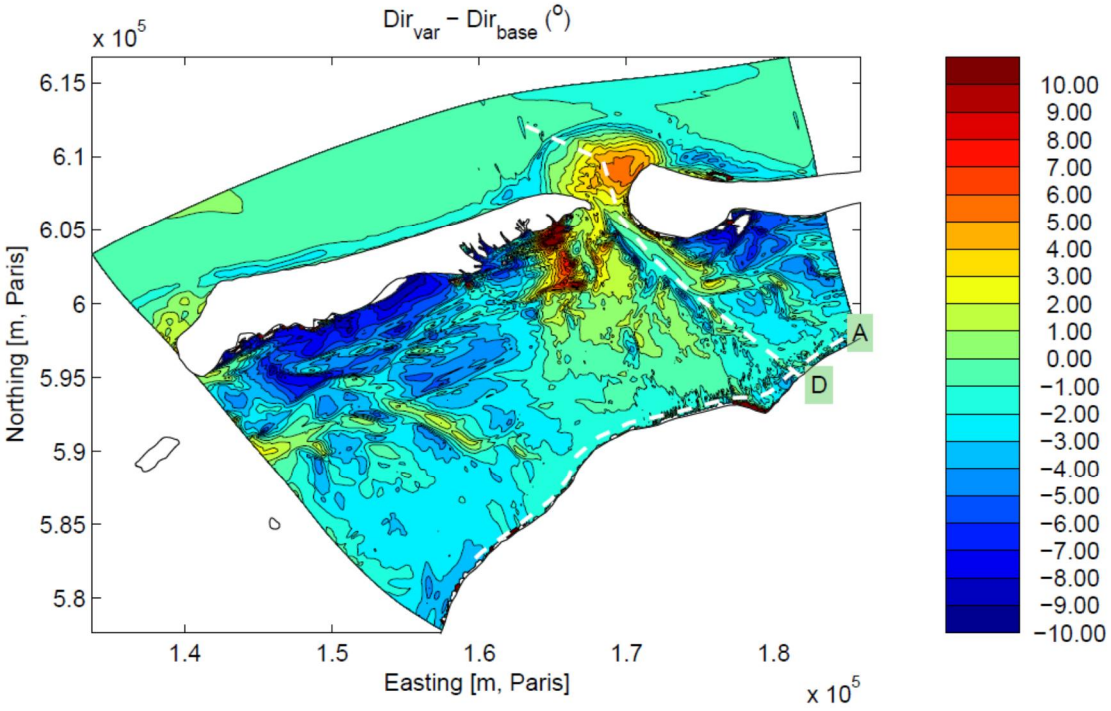

Figure 4.3 Differences in mean wave direction for an increase in water level of 1 m during an extreme NW storm (wind direction = 315°, U_{10} = 34 m/s, water level = 5.7 m+NAP, $H_{m0\_boundary}$ = 9,4 m, $T_{p\_boundary}$ = 18 s). As presented in WL & Alkyon (2007).

Wind direction

By contrast, as the waves in the tidal inlet are mainly locally generated, they prove to be very sensitive to variations in wind direction; a change of 10° in wind direction results in a 10° difference in wave direction at the output locations along the coast, see Figure 4.4, where the wind direction was changed by -10°. Also, the directional spreading in the inlet changes significantly, as can be seen in Figure 4.5.

Currents

The wave direction along the coast is also affected by local currents. Figure 4.6 shows an example of the differences in mean wave direction that can be seen when the currents (during ebb) are deactivated. The largest differences are seen in the ebb tidal channels and on some of the tidal flats with up to 10° difference in mean wave direction. However, near the coast the differences due to the deactivation of the current are smaller (circa 3-4 degrees).

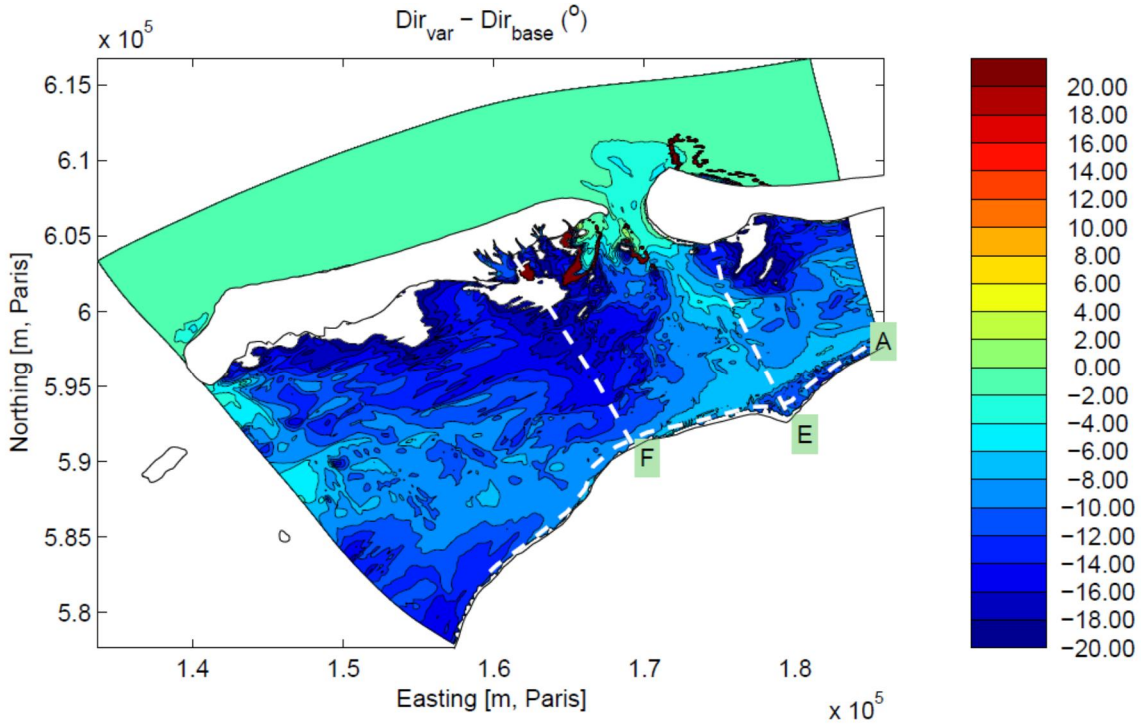

Figure 4.4 Differences in mean wave direction for a -10^o variation in wind direction during a severe historical NW storm (8-2-2004, 22:30, wind direction = 325^o, U_{10} = 16.6 m/s, water level = 2.6 m+NAP, $H_{m0\_boundary}$ = 5.3 m, $T_{m-1,0\_boundary}$ = 9.5 s, wave direction at the boundary = 319^o). As presented in WL & Alkyon (2007).

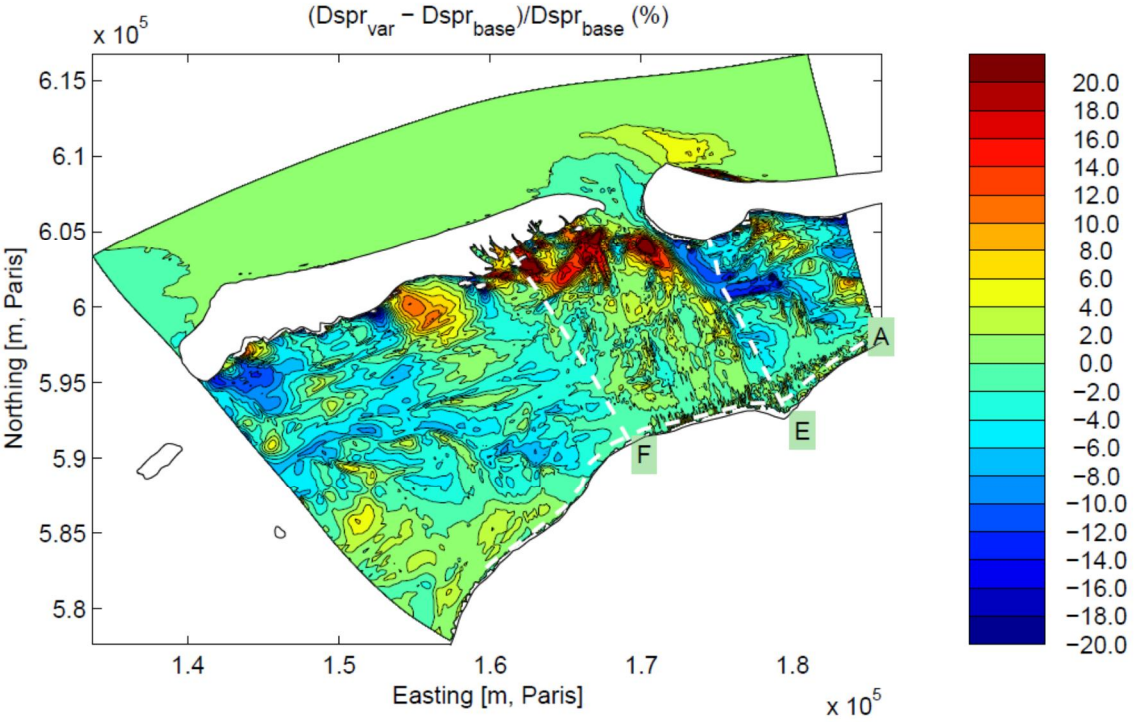

Figure 4.5 Differences in directional spreading for a -10^o variation in wind direction during a severe historical NW storm (8-2-2004, 22:30, wind direction = 325^o, U_{10} = 16.6 m/s, water level = 2.6 m+NAP, $H_{m0\_boundary}$ = 5.3 m, $T_{m-1,0\_boundary}$ = 9.5 s, wave direction at the boundary = 319^o). As presented in WL & Alkyon (2007).

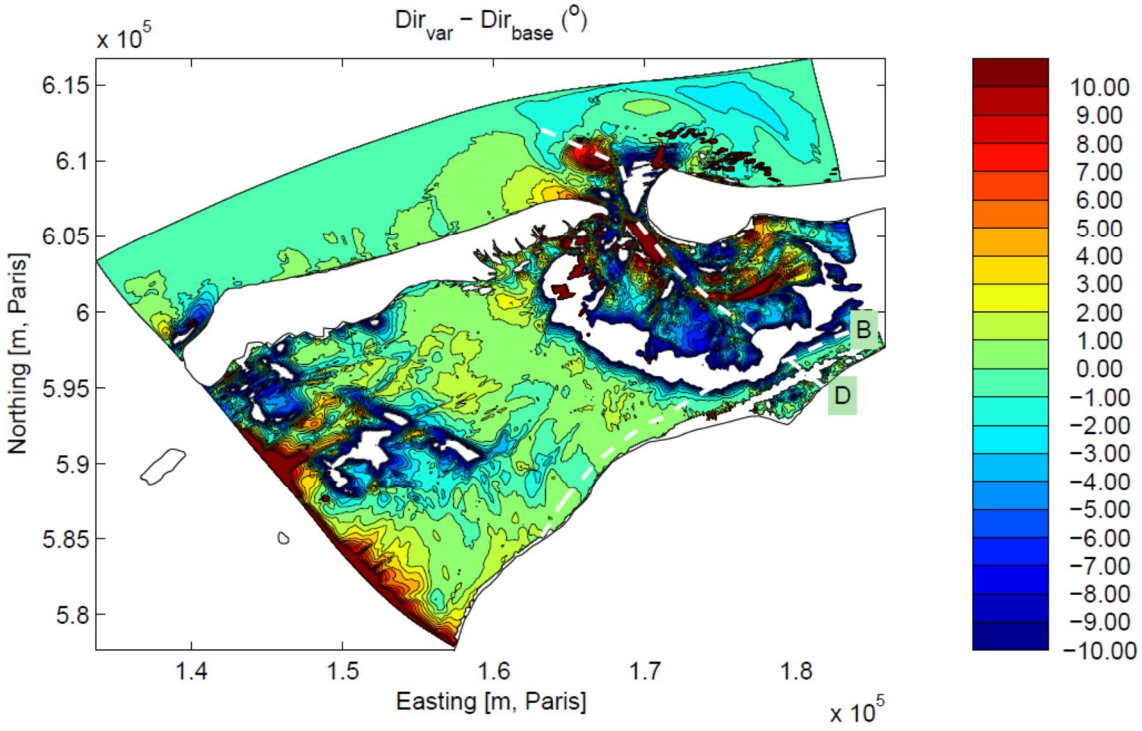

Figure 4.6 Differences in mean wave direction when the ebb current is deactivated during a severe historical NW storm (9-2-2004, 1:30, wind direction = 328°, U_{10} = 16.3 m/s, water level = 1.75 m+NAP, $H_{m0\_boundary}$ = 4.8 m, $T_{m-1,0\_boundary}$ = 9.7 s, wave direction at the boundary = 338°). As presented in WL & Alkyon (2007).

Physical processes

The region of the ebb tidal delta is affected most by variations in the strength of depth-induced breaking and triad interactions. The ebb tidal delta dissipates a substantial amount of wave energy arriving from the North Sea. Therefore, inside the Wadden Sea locally generated waves dominate under depth-limited conditions. Closer to the coast, saturated surf zone conditions exist, which further limit the wave heights. For the hypothetical extreme storms considered in WL & Alkyon (2007), these depth-limited conditions exist over almost the entire Wadden Sea interior behind the Amelander Zeegat. The saturated conditions significantly restrict the sensitivity of model results at the sea defences to the investigated variations. The mean wave direction near the Frisian coast shows the largest sensitivity of all physical processes to the bottom friction. A change of -50% in the bottom friction results in a 3° more northerly mean wave direction.

4.3 Analysis wave conditions Wadden Sea and Western Scheldt during extreme storms

WL & Alkyon (2007) showed that the wave conditions along the Frisian coast behind Ameland during extreme storms are not very sensitive to variations in model output or model settings in other parts of the inlet. However, it is plausible that at places in the Wadden Sea and the Western Scheldt where the tidal inlets are wider, and where the foreshore is steeper (e.g. when the tidal channel runs close to the mainland), saturated conditions may not occur and a larger model sensitivity than that demonstrated in WL & Alkyon (2007) could be found.

Furthermore, the wave conditions along the Frisian coast behind the Amelander Zeegat were predominantly wind-sea, even during extreme events. However, at some places in the Wadden Sea and the Western Scheldt the wave penetration of swell waves may be larger. At

these places it could be possible that the results of WL & Alkyon (2007) are not applicable and that the wave direction near the coast is more sensitive to model inputs and physics.

To investigate whether other areas in the Wadden Sea will be more sensitive to variations in the mean wave direction during extreme storm conditions, the H_{m0}/Depth ratios of different extreme storm cases from the CR-2011 database were studied (described in Svašek Hydraulics/HKV Lijn in Water, 2011a,b). In addition, the low-frequency wave penetration in the Wadden Sea and Western Scheldt is studied by presenting the low-frequency wave height (H_{E10}) along the coast.

It should be noted that the findings in this section should be handled with care, as all conclusions are solely based on SWAN computations. From various existing hindcasts we know that the low-frequency energy is often underestimated by SWAN. Therefore, low-frequency wave penetration near the coast could be larger during extreme storms than shown in this section. However, since wave measurements of low-frequency wave energy are limited near the coast, it is not possible to make a better estimation of the low-frequency energy near the coast than the estimation that is made with SWAN.

H_{m0}/Depth ratios

The H_{m0}/Depth ratios were studied with case G2U35D330P00S20T03 from the CR-2011 database (Wadden Sea grid, wind speed 35 m/s, wind direction 330^{o}N, no phase difference between the tidal peak and the wind peak, water level set-up 2m at the peak of the storm). This case is comparable to the extreme NW storm case that was studied in WL & Alkyon (2007). The wave conditions are depth-limited when the H_{m0}/Depth ratio is 0.4 or larger (criterion WL & Alkyon, 2007).

The H_{m0}/Depth ratios are shown in Figure 4.7. It can be seen that the wave conditions in case G2U35D330P00S20T03 are depth-limited at the Amelander Zeegat coast. However, it can be seen that the tidal channels in some of the tidal inlets (e.g. Marsdiep, Eierlandse gat, Friesche Zeegat and the Eems-estuary) run close to the dikes. In these situations the conditions are not depth-limited and waves can become higher and the wave conditions are probably more sensitive to some of the model physics. Furthermore, wave penetration of low-frequency energy can be significant in these areas.

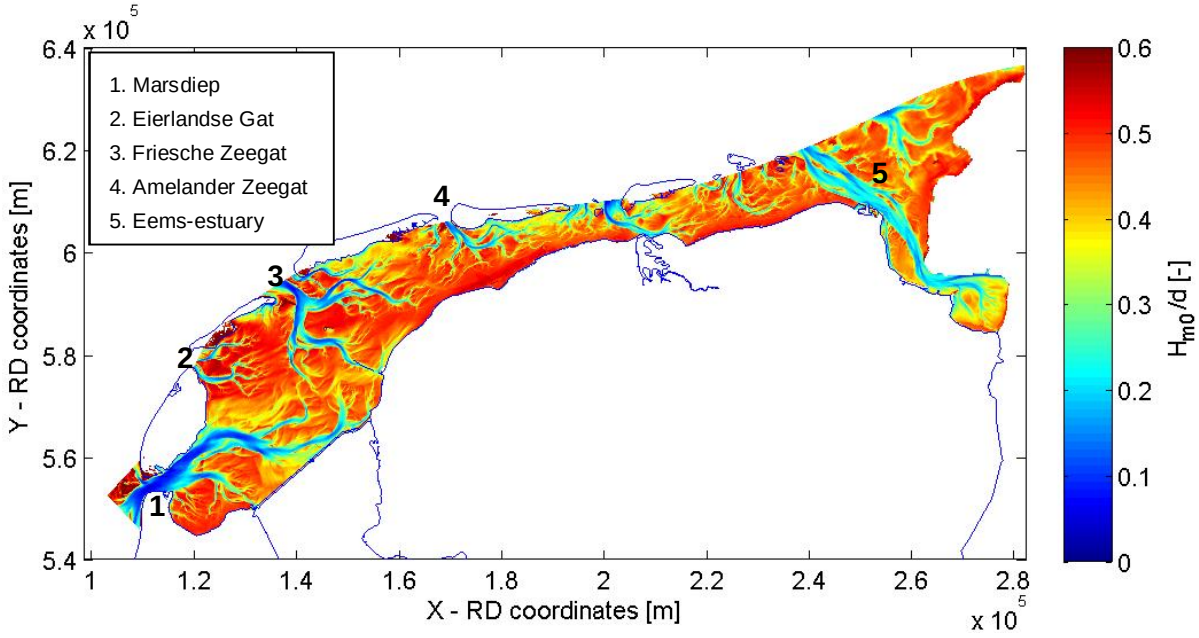

Figure 4.7 *H_{m0}/depth ratio in the Wadden Sea for case G2U35D330P00S20T03 from the CR-2011 database (Wadden Sea grid, wind speed 35 m/s, wind direction 330°N, no phase difference, water level set-up 2m, at the peak of the storm).*

Low-frequency wave penetration

The low-frequency penetration during extreme events has been studied in the Wadden Sea and the Western Scheldt. In Figure 4.8 and Figure 4.9 the low-frequency wave height (H_{E10}) for the Wadden Sea cases XXU35DXXXP00S20T03 and XXU40DXXXP00S40T03 from the CR-2011 database is shown. The X indicates that a number of different values have been used in the analysis; the information of grids G2, G3 and G4 were used and the wind directions from 210:30:360 degrees were analysed. In addition in Figure 4.10 the wave penetration for the cases G1U35DXXXP00S20T03 in the Western Scheldt is shown. For every Hydra-K output location the cases with the largest H_{E10} have been presented. The H_{E10} is a good measure to show the wave penetration of waves with frequencies smaller than 0.1 Hz at the output locations along the dikes.

There are certain locations along the coast where the low-frequency wave penetration is high, as can be seen in Figure 4.8, Figure 4.9 and Figure 4.10. In Figure 4.8, the areas where low-frequency energy penetrates towards the coast are limited to the island heads of Texel and Ameland, close to Lauwersoog and in the Eems-estuary. However, with a higher water level set-up, more wave energy penetrates towards the coast, see Figure 4.9. It should be noted that the coast behind the Amelander Zeegat seems unaffected by low-frequency penetration, even in this extreme case.

In Figure 4.10 it can be seen that there is limited low-frequency wave penetration into the Western Scheldt, even in an extreme event. Low-frequency waves higher than 0.5 metres do not penetrate further into the Western Scheldt than the harbour of Vlissingen. However, in the mouth of the Western Scheldt the H_{e10} is significant.

These findings are important, since many conclusions in the previous chapters on the validity of the SWAN wave directions near the coast were based on situations where the wave penetration is limited and locally wind-generated waves dominate. It was seen that in these

cases the error in wave direction near the coast can be linked to errors made in the wind direction and to a small extend to errors in the model physics. However, in cases where the wave penetration is high, errors in wave direction will be higher, for example due to errors in the modelled nonlinear interactions and the currents. It is expected that the directional error in cases with high low-frequency wave penetration will be in the order of the errors found in the tidal channels (see Chapter 2). However, it is hard to verify this as only limited directional measurements are available at locations close to the coast where high low-frequency wave penetration could be expected (UHW1 & WRW1 during the November 2007 storm).

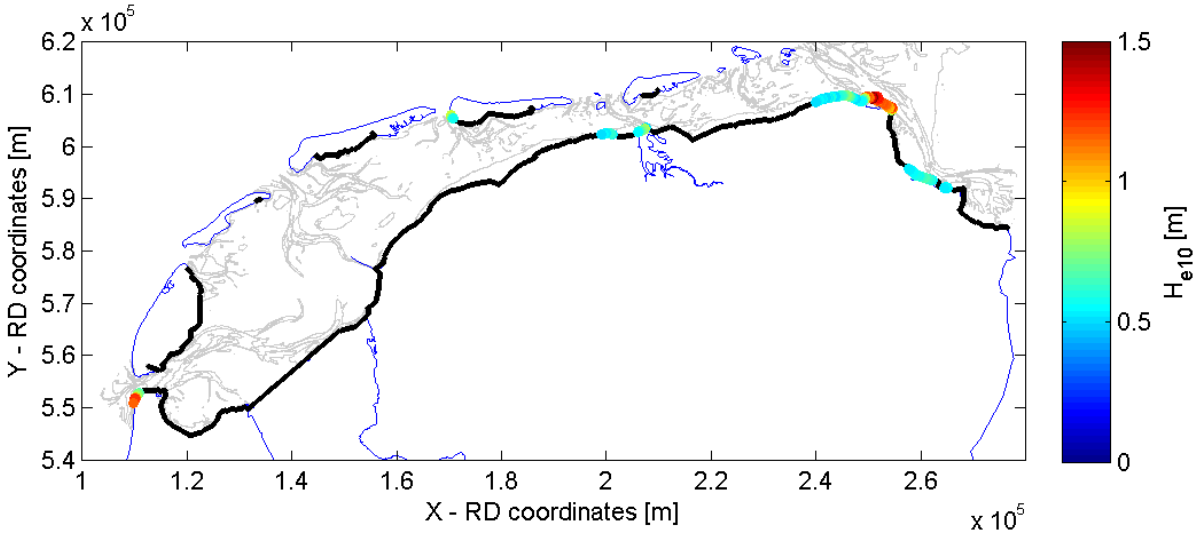

Figure 4.8 *Highest penetration of low-frequency energy < 0.1 Hz (H_{e10}) for extreme storms in the CR-2011 database along the Wadden Sea coastline during wind speeds of 35 m/s (XXU35DXXXP00S20T03, all wind directions have been analysed, no phase differences, water level set-up 2 m, at the peak of the storm). H_{e10} < 0.5 m are not shown, black dots indicate the Hydra-K output locations.*

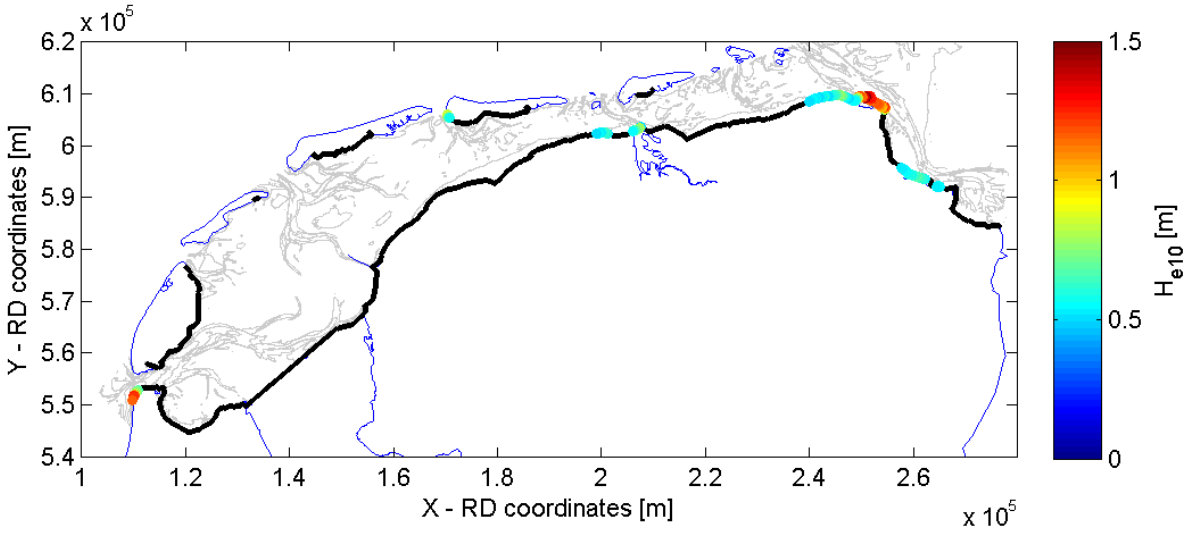

Figure 4.9 *Highest penetration of low-frequency energy < 0.1 Hz (H_{e10}) for extreme storms in the CR-2011 database along the Wadden Sea coastline during wind speeds of 40m/s (XXU40DXXXP00S40T03, all wind directions have been analysed, no phase differences, water level set-up 4 m, at the peak of the storm). H_{e10} < 0.5 m are not shown, black dots indicate the Hydra-K output locations.*

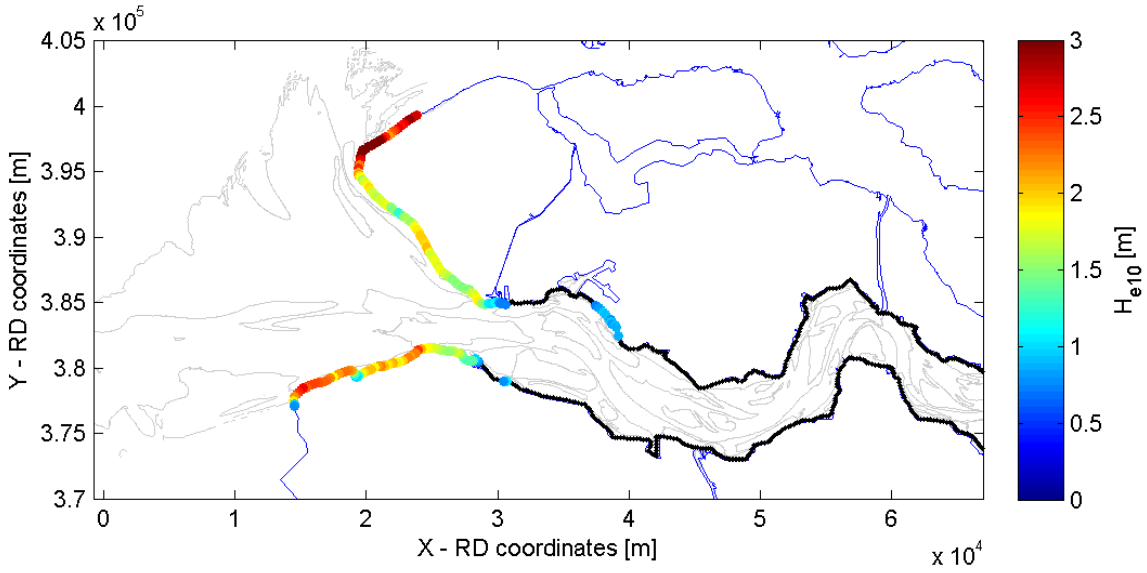

Figure 4.10 Highest penetration of low-frequency energy < 0.1 Hz (H_{e10}) for extreme storms in the CR-2011 database along the Wadden Sea coastline during wind speeds of 35 m/s (G1U35DXXXP00S20T03, all wind directions have been analysed, no phase differences, water level set-up 4 m, at the peak of the storm). H_{e10} < 0.5 m are not shown, black dots indicate the Hydra-K output locations.

4.4 Conclusions and recommendations

4.4.1 Conclusions

- WL & Alkyon (2007) demonstrated that simulated wave directions at the sea defences are very sensitive to the wind direction.
- WL & Alkyon (2007) showed that the wave conditions along the Frisian coast behind Ameland during extreme storms are not very sensitive to variations of the model input or physics in other parts of the inlet, as the waves in a large part of the Amelander Zeegat are locally generated wind waves and depth-limited.
- However, at places in the Wadden Sea where the tidal inlets are wider and where the foreshore is steeper (e.g. when the tidal channel runs close to the mainland), a greater model sensitivity to model inputs and physics than that demonstrated in WL & Alkyon (2007) is expected, based on the H_{m0}/depth ratios in the Wadden Sea during an extreme NW event.
- Furthermore, high low-frequency wave penetration is expected at a number of locations along the Wadden Sea coast during extreme storm events, based on SWAN results from the CR-2011 database. At these locations it is expected that errors in wave direction will be higher, for example due to errors in the modelled nonlinear interactions and the currents.

4.4.2 Recommendations

More directional wave measurements are needed to confirm the results presented in this chapter. Areas of interest for directional measurements are the new ‘stroommeetpaal Eemshaven’ (SPE) or the measurement location Uithuizerwad (UHW) or the Wierumerwad (WRW) measurement location. As the water depth at these locations is a very important factor it is also necessary to measure the water level at these locations.

5 An indication of the error in required crest height due to possible errors in wave direction

5.1 Introduction

In the previous chapters it was concluded that the locations in the Wadden Sea where the largest errors in hydraulic loads/required crest height due to inaccurate wave directions are expected are the areas where:

- The angle of wave attack is larger than circa 75^{o} (chapter 3);
- A high low-frequency wave penetration is expected (chapter 4).

In this chapter an attempt is made to give an indication of the error in required crest height due to possible errors in wave direction, based on the conclusions of chapters 3 and 4, the error statistics for nearshore locations of chapter 2 and the sensitivity of the required crest height to errors in wave direction (Section 3.2.2). This is done for the Wadden Sea.

For the Western Scheldt it is hard to give a similar indication, since the comparison between the computed and measured wave directions is only based on two locations. Much smaller errors are seen at the location near the coast Cadzand than were seen in the Wadden Sea, but it is unknown whether this is true for all locations in the Western Scheldt.

5.2 Error in required crest height (RCH) in the Wadden Sea

Table 5.1 gives an indication of the error in required crest height due to errors in the wave direction in the Wadden Sea. The magnitude of the error in required crest height is depending on the angle of wave attack; Section 3.2 showed that the required crest height is very sensitive when the angle of wave attack is larger than ca. 75 degrees. Furthermore, the expected error in nearshore wave direction depends on whether the waves consist of wind-sea or a combination of wind-sea and swell. For the latter it is expected that the errors will be larger, see Section 3.3 and Chapter 4. The errors in required crest height are indicative only, as only a limited number of locations have been studied. The sensitivity of the crest height to the angle of wave attack (β) may be different at locations that were not considered. Furthermore, since the bias and standard deviation of the computed wave directions are based on only a few directional measurements along the Wadden Sea coast, the accuracy of these values is limited. Therefore, Table 5.1 should merely be seen as a rough indication of the error in required crest level that may occur.

	Wind-sea error in wave direction: 10^o bias and 5^o std[1]	**Wind-sea and swell** error in wave direction: 17^o bias and 5^o std[2]
β **< 75^o** sensitivity RCH to β: ca. 10 cm/10^o (par 3.2.2)	0-20 cm error in RCH 0-3% rel. error in RCH[3]	0-35 cm error in RCH 0-4% rel. error in RCH[3]
β **> 75^o** sensitivity RCH to β: ca. 30 cm/10^o (par 3.2.2)	20-40 cm error in RCH 3-5% rel. error in RCH[3]	35-70 cm error in RCH 4-9% rel. error in RCH[3]

Table 5.1 An indication of the error in required crest height (RCH) due to possible errors in wave direction in the Wadden Sea. The error is based on the range of μ-2σ to μ+2σ, where μ is the bias and σ the standard deviation (std). β is the angle of wave attack relative to the dike normal.

[1]) roughly based on the statistics of par. 2.2.2 and 2.3.2 (locations AZB52 and PBW1).

[2]) roughly based on par 2.3.2 (locations UHW1, WRW1)

[3]) this relative error concerns an example for a required crest height of 8 m+NAP.

Figure 5.1 shows where the conditions described in Table 5.1 occur. Locations where no low-frequency wave penetration is expected are shown in green. Locations where low-frequency wave penetration is expected during an extreme event are shown in red for an extreme storm with a wind speed of 35 m/s and a set-up of 2 m. Finally, locations where the wave angle of attack is more than 60^o are shown in black.

Locations that are only green have a small error in crest height due to errors in wave direction, see Table 5.1, first column, first row. When a black marker is added to the green marker, the second row of the first column applies. Locations that are only marked with a red marker are likely to have larger errors in crest heights due to errors in wave direction, see Table 5.1, second column, first row. When the red markers are also marked with a black marker, the errors in crest heights due to errors in wave direction are largest and the second row of the second column applies.

The areas in Figure 5.1 that are both marked with a red marker and a black marker include:

- The area near Eemshaven;
- The area near Delfzijl;
- The area near Lauwersoog;
- The western head of Ameland.

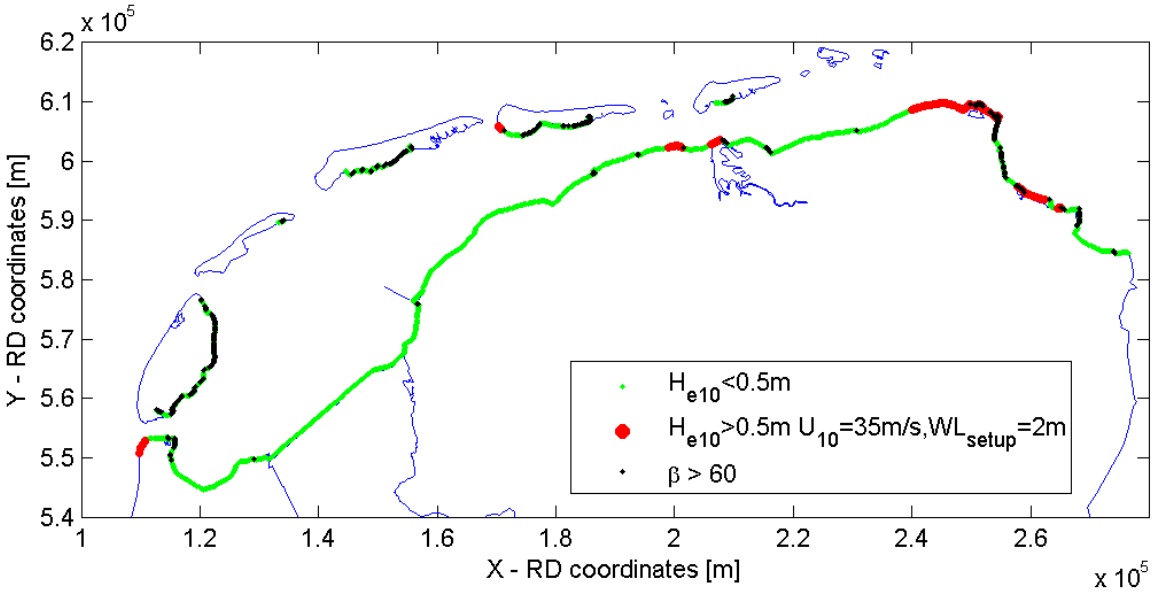

Figure 5.1 Overview of locations where (in green) no l-f wave penetration is expected, (in red) significant low-frequency wave penetration is expected during an extreme event, with a wind speed of 35 m/s and a set-up of 2 m and (in black) the wave angle of attack is more than 60°.This information is extracted from the CR-2011 database.

During swell events, the significant wave height and period near the coast could also be less reliable due to local errors in modelled wave direction (in the ebb-tidal delta or channels). These errors have not been addressed in this study and it is referred to Deltares (2014a) for an analysis of the effect of local errors in modelled wave direction on the significant wave height and wave period.

The results in this chapter show that the errors in required crest height due to an error in the wave direction can be significant in some cases, particularly when the angle of wave attack is larger than 75° and a high amount of low-frequency wave penetration is expected. Thus, for these cases the error in wave direction cannot be neglected. Errors of up to 70 centimetres for the required crest height are in line with the model uncertainties for significant wave height and mean wave period specified for WTI-2017 in Deltares (2015). In WTI-2017 a relative standard deviation (σ) of 0.19 was specified for the significant wave height and a σ of 0.11 was specified for the mean wave period. However, it should be noted that the values given for WTI-2017 are global values (valid for the whole area), whereas errors in required crest height due to errors in wave direction are local errors and cannot be used for the whole area.

Further steps are needed to determine the uncertainty in the wave direction, according to Deltares (2015) (for example with an adjunct model) or determine a fallback option in case large errors in required crest height are expected. It must be noted that first more directional wave measurements are needed in order to be able to obtain reliable estimates of the uncertainties in the wave directional errors.

6 Conclusions and recommendations

6.1 Introduction

In this report the SWAN performance in complex tidal inlet systems regarding wave directions during storm conditions was studied. In addition, it was investigated what the SWAN accuracy concerning wave directions implies for the hydraulic loads and the required crest height. In this chapter the main conclusions of the previous chapters are summarized and recommendations are given.

6.2 Statistical analysis SWAN wave direction

The SWAN performance with respect to the wave direction has been assessed, based on results of existing hindcast studies in the Amelander Zeegat, the Eastern Wadden Sea and the Western Scheldt.

It was concluded that SWAN in the Wadden Sea often predicts a too northerly mean wave direction and often underestimates the directional spreading. In the Western Scheldt no clear bias is seen and also the bias in the directional spreading is limited. However, the number of directional measurement locations in the Western Scheldt is limited to two locations: one location west of the ebb-tidal delta (DELO) and one location located in the southern channel close to the coast of Cadzand (CADW). Therefore, the conclusions of the error statistics in the Western Scheldt are probably not representative for the whole Western Scheldt. For this reason only the conclusions of the error statistics of the mean wave direction in the Wadden Sea are presented here.

On the North Sea side of the ebb-tidal delta SWAN predicts the mean wave direction and directional spreading very well, with on average less than 5 degrees deviation. In the tidal channels the model performance with respect to wave directions is worst. In previous studies this was related to the fact that SWAN does not model the sub-harmonic nonlinear interactions that broaden the directional spectrum. Therefore, the waves are refracted differently, when encountering tidal channels. In addition, currents play a role, as was shown in previous hindcasts.

Close to the coast there are limited directional measurements available. However, the few observations show that a model bias of 10 to 20 degrees in the mean wave direction is likely with a standard deviation of circa 5 degrees. In addition, the directional spreading is underestimated with 10 to 20 degrees and a standard deviation of a few degrees. The agreement between the computed and measured mean wave directions is lower in cases where low-frequency wave penetration is measured than in cases where windsea predominates.

6.3 Sensitivity of hydraulic loads to the wave direction

The question is addressed how sensitive the hydraulic loads and the required crest levels are to the nearshore wave direction. This has been checked by studying the sensitivity of the wave overtopping calculations in Hydra-K to changes in wave direction, using the CR-2011 database for the Eastern Wadden Sea. The sensitivity analysis showed that the effect of an error in the wave direction is largest when the waves are slanting (more than 75^{o}). In these cases an error of 10 degrees in wave direction could result in an error in crest height of circa 30 centimetres. In contrast, in cases were the angle of wave attack is close to normal (less than 75^{o}): an error of 10 degrees in the wave directions results in an error in crest height of 7-

10 centimetres. The values presented here are indicative, as only three locations were considered in the sensitivity analysis. Locations with slanting wave directions during normative conditions occur at the southern side of the islands of Ameland and Schiermonnikoog as well as in the Eems Dollard and inside the Western Scheldt.

In addition it was shown that simulated wave directions at the sea defences are very sensitive to directional information in the imposed wind fields. At places in the Wadden Sea where the tidal inlets are wide, and where the foreshore is steep (e.g. when the tidal channel runs close to the mainland), high low-frequency wave penetration is expected during extreme storm events. At these locations it is expected that errors in wave direction will be high, for example due to errors in the modelled nonlinear interactions and the currents. Locations where high low-frequency energy wave penetration near the coast can be expected during extreme storm condition are the island heads of Texel and Ameland, near Lauwersoog and in the Eems-estuary. It should be noted that these findings should be handled with care, as all conclusions are solely based on SWAN computations.

Furthermore, it was seen that the hydraulic loads seem to be very sensitive to the inclusion of a secondary wave direction in the load function when the angle of wave attack relative to the dike normal is larger than 75^{o}.

6.4 An indication of the error in required crest height

Based on the analyses performed in this report, it can be concluded that the locations where the largest errors in hydraulic loads are expected are the areas in tidal inlets where:

- The angle of wave attack is large;
- And a high low-frequency wave penetration is expected.

An indicative maximum error in required crest height of plus or minus 35 to 70 centimetres could be expected, in case both aspects occur.

Thus, areas with potentially large errors in crest height due to errors in wave direction include:

- The area near Eemshaven;
- The area near Delfzijl;
- The area near Lauwersoog;
- The head of Ameland.

It depends on the area and the orientation of the flood defence whether the calculated required crest heights will be too low or too high due to errors in wave direction. Also, the error analysis could be less reliable for the head of Ameland, as the error statistics could be different in these areas.

It is hard to give a similar indication for the Western Scheldt, since the comparison between the computed and measured wave directions is only based on two locations. Much smaller errors are seen at the location near the coast of Cadzand than were seen in the Wadden Sea, but it is unknown whether this is true for all locations in the Western Scheldt.

Errors of up to 70 centimetres for the required crest height are in line with the model uncertainties for significant wave height and mean wave period specified for WTI-2017 in Deltares (2015). However, it should be noted that the values given for WTI-2017 are global values (valid for the whole area), whereas errors in required crest height due to errors in wave direction are local errors and cannot be used for the whole area.

6.5 Recommendations

It is recommended to study the areas with potentially large errors in crest height, as identified in this study, extra carefully in the next WTI assessment. Further steps are needed to determine the uncertainty in the wave direction, according to Deltares (2015) (for example with an adjunct model) or determine a fallback option in case large errors in required crest height are expected. More directional wave measurements are required to confirm the results presented in this report. Areas of interest for directional measurements are the new 'stroommeetpaal Eemshaven' (SPE) or the measurement location Uithuizerwad (UHW) or the Wierumerwad (WRW) measurement location. As the water depth at these locations is a very important factor it is also necessary to measure the water level at these locations.

In addition, it should be noted that it is planned to use time evolving storms in the future to determine the HBC and this will possibly involve non-stationary SWAN runs and hydrodynamic coupling. In the tidal channels, tidal currents and changing water levels potentially give rise to non-stationary effects that could have a significant impact on model results, including directional properties. Therefore, in case non-stationary SWAN runs will be used in future HBC rounds, it is worth reconsidering the directional performance of SWAN.

Furthermore, more research is necessary into the effect of bi- or multi modal sea states on the hydraulic loads.

In this study the influence of wave direction on required crest height is assessed for only three locations. For a more reliable result it is advised to perform a more thorough sensitivity analysis in which more locations are considered.

As mentioned in the scope the area of interest of this study is limited to the Wadden Sea and Western Scheldt. The findings therefore concern only these areas and are not directly applicable to other areas. For other areas it is suggested to look for local directional observations or observations that reflect the local conditions and to look for specific areas where errors in wave direction can be expected for instance due to slanting waves and/or the presence of swell.

7 References

Alkyon (2007a). Analysis SWAN hindcast tidal inlet of Ameland. Storm events of 8 February 2004 and 2, 8 January 2005. ref A1725R4, February 2007.

Alkyon (2007b). Analysis SWAN hindcast tidal inlet of Ameland. Storms of 17 December 2005 and 9 February 2006. ref A1725R5, February 2007.

Alkyon (2008). SWAN hindcast in the Eastern Wadden Sea and Eems-Dollard estuary, storm of 9 November 2007. ref A2191, December 2008.

Booij, N., R.C. Ris and L.H. Holthuijsen (1999). A third generation wave model for coastal regions, Part I, Model description and validation, J. Geophys. Res., 104, C4, 7649-7666.

Bouws, E. and G. J. Komen (1983). On the balance between growth and dissipation in an extreme, depth-limited wind-sea in the southern North Sea. J. Phys. Oceanogr., 13, 9, 1653-1658.

Deltares (2010). Wave propagation under influence of currents. Deltares report 1202119-003-HYE-0002, November 2010.

Deltares (2011). Improvements in spectral wave modelling in tidal inlet seas: overview of results of the SBW-Waddenzee project 2006-2010. Deltares report 1202119-006-HYE-0003, May 2011.

Deltares (2014a). Modelling of wave penetration in complex areas: analysis of hindcast data, WTI – Hydraulische belastingen. Deltares report 1209433-007-HYE-0006, December 2014.

Deltares (2014b). SWAN hindcasts Wadden Sea, December 2013. Tidal inlet of Ameland and eastern Wadden Sea. Deltares report 1209433-007-HYE-0005, October 2014.

Deltares (2015). Modelonzekerheid belastingen. Wettelijk Toetsinstrumentarium WTI-2017. Deltares report 1209433-008-HYE-0007, June 2015.

Eldeberky, Y. (1996). Nonlinear transformation of wave spectra in the nearshore zone. Ph.D. thesis, TU Delft, 203 pp.

Groeneweg, J., van Gent, M., van Nieuwkoop, J., and Toledo, Y. (2015). Wave Propagation into complex coastal systems and the role of nonlinear interactions. J. Waterway, Port, Coastal, Ocean Eng., 10.1061/(ASCE)WW.1943-5460.0000300, 04015003.

Groeneweg, J., J. van Nieuwkoop and Y. Toledo (2014b). On the modelling of swell wave penetration into tidal inlets. In Proceedings of the International Conference on Coastal Engineering, Seoul, Korea.

Hasselmann, S., K. Hasselmann, J. A. Allender, and T. P. Barnett (1985). Computations and parameterizations of the nonlinear energy transfer in a gravity-wave spectrum. Part 2: parameterization of the nonlinear transfer for application in wave models, J. of Phys. Oceanogr. 15, 1378-1391.

Herbers, T. H. C., S. Elgar, and R. T. Guza (1995), Generation and propagation of infragravity waves, J. Geophys. Res., 100 (C12), 24863–24872, doi:10.1029/95JC02680.

Kuik, A.J., G.Ph. van Vledder, and L.H. Holthuijsen, 1988: A method for the routine analysis of pitch-and-roll buoy wave data, Journal of Physical Oceanography, Vol. 18, No. 7, 1024-1034.

Krogstad HE (2001) Second order wave spectra and heave/slope wave measurements. In: Proc. Symp WAVES 2001, San Francisco, 2–6 September 2001

Royal Haskoning (2008). Hindcast tidal inlet of Ameland storms January and March 2007. Royal Haskoning Report 9T5842.A0, October 2008.

Smale, A. en I. Wenneker (2011). Twee-dimensionale golfspectra. Memo SBW Informatiebehoefte, Veldmetingen en Data, 31 mei 2011, 1204207-004-HYE-0005.

Svasek Hydraulics/HKV Lijn in Water (2011a). Productieberekeningen Waddenzee WTI 2011: rapportage fase 1. Svasek Hydraulics/HKV Lijn in water report 1.1/1. May 2010.

Svasek Hydraulics/HKV Lijn in Water (2011b). Productieberekeningen Westerschelde WTI 2011: rapportage fase 1. Svasek Hydraulics/HKV Lijn in water report 2.1/1. Februari 2010.

TAW (2002). Technisch Rapport Golfoploop en Golfovelsag bij Dijken. Technische Adviescommissie voor de Waterkeringen, Delft, May 2002.

Van der Westhuysen, A. J., M. Zijlema, and J. A. Battjes (2007). Nonlinear saturation-based whitecapping dissipation in SWAN for deep and shallow water. Coastal Engineering 54, 151-170.

Van der Westhuysen, A. J. (2007). Nonlinear saturation-based whitecapping dissipation in SWAN for deep and shallow water. Coastal Engineering, Vol. 54, 151-170, doi:10.1016/j.coastaleng.2006.08.006.

Van der Westhuysen, A. J. (2009). Modelling of depth-induced wave breaking over sloping and horizontal beds. 11th International Workshop on Wave Hindcasting and forecasting 2009 (pp 1-10).

Van der Westhuysen, A. J. (2010). Modeling of depth-induced wave breaking under finite depth wave growth conditions. Journal of Geophysical Research, Vol. 115, C01008, 2010.

Van der Westhuysen, A. J. (2011). Spectral modeling of wave dissipation on negative current gradients. *J. Geophys. Res*., Vol. 68, 17-30, doi:10.1016/j.coastaleng.2012.05.001.

Wenneker, I., Kieftenburg, A.T.M.M. Westhuysen, A.J. van der and L. Verhage (2009). SWIVT, an instrument for validation and testing of SWAN . Coastal Engineering 2008: proceedings of the 31st international conference (Hamburg, 13 August – 5 September 2008), vol. 1 ; p. 509-520

Witteveen & Bos (2008). Hindcast of the 8 and 9 november 2007 storm for the tidal inlet of Ameland. DT293-2/winb/011, November 2008.

Witteveen+Bos (2010): Hindcast verification of SWAN in the Western Scheldt. ref DT311-1, March 24 2010.

WL & Alkyon (2007a). Storm hindcast for Wadden Sea, Hindcasts in inlet systems of Ameland and Norderney and Lunenburg Bay. WL | Delft Hydraulics Report H4918.20, September 2007.

WL&Alkyon (2007b). Sensitivity analysis of SWAN for the Amelander Zeegat. WL | Delft Hydraulics Report H4918.41, September 2007.

A Statistical error analysis

The error statistics that have been used in Chapter 2 are described in this Appendix. In the error analysis it has been taken into consideration that the mean wave direction and the directional spreading are circular data. The calculation has been done with the ORCA matlab toolbox.

Every observation is considered as unit vector and vector addition has been applied to compute averages of angles. The sample mean direction $\bar{x}$ is determined as follows:

$$\bar{x} = \tan^{-1}\left({}^{S_n}/_{C_n}\right)$$

Where $S_n = 1/n \sum_{i=1}^{n} \sin x_i$, and $C_n = 1/n \sum_{i=1}^{n} \cos x_i$, in the range [0,2π]. The bias is computed by substituting x_i for $y_i - x_i$ in the formula above, where x_i are the measurements and y_i the SWAN results. The variance is defined as:

$$S_0 = 1 - \sqrt{\left({C_n}^2 + {S_n}^2\right)}$$

The circular standard deviation (σ) is calculated as follows:

$$\sigma = \left(-2 \cdot ln(1 - S_0)\right)^{\frac{1}{2}}$$

And the circular root-mean-square error (RMSE) is defined as:

$$RMSE = \sqrt{-2 \cdot ln\left(\frac{1}{n}\sum_{i=1}^{n} \cos(x_i - y_i)\right)}$$